AMEGHINIANA
A GONDWANAN PALEONTOLOGICAL JOURNAL

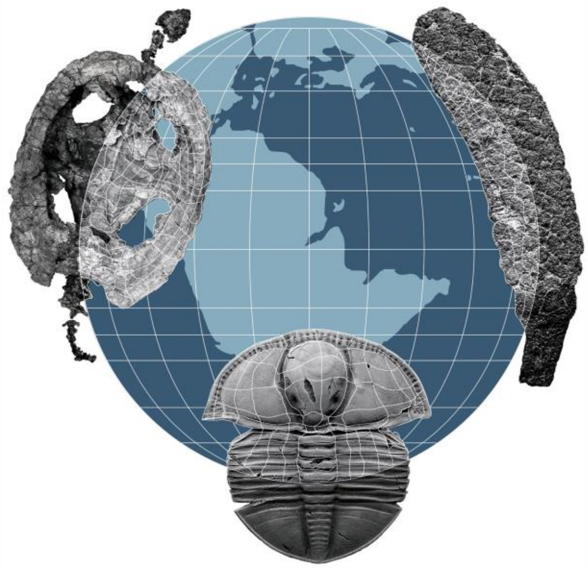

Submitted: April 11th, 2016 – **Accepted**: September 11th, 2016

To link and cite this article:

doi: 10.5710/AMGH.11.09.2016.3011

THE POSTCRANIAL SKELETON OF THE LOWER JURASSIC *TRITYLODON LONGAEVUS* FROM SOUTHERN AFRICA

EL ESQUELETO POSTCRANEANO DE *TRITYLODON LONGAEVUS* DEL JURÁSICO INFERIOR DE ÁFRICA DEL SUR

LEANDRO C. GAETANO

Departamento de Ciencias Geológicas, FCEyN, Instituto de Estudios Andinos "Don Pablo Groeber" – IDEAN (Universidad de Buenos Aires-CONICET), Ciudad Autónoma de Buenos Aires, Argentina

Evolutionary Studies Institute, University of the Witwatersrand, Johannesburg, South Africa

lcgaetano@gl.fcen.uba.ar

FERNANDO ABDALA

Evolutionary Studies Institute, University of the Witwatersrand, Johannesburg, South Africa

ROMALA GOVENDER

Iziko Museums of South Africa, Cape Town, South Africa

50 pages (text-references), 13 figures, 6 tables

Cabezal: GAETANO ET AL: POSTCRANIUM OF THE CYNODONT *TRITYLODON LONGAEVUS*

Corresponding author: Leandro C. Gaetano

Abstract. *Tritylodon longaevus* is one of the most common members of the Lower Jurassic faunas of the Karoo Basin. The cranial and dental anatomy of this taxon is well known, but its postcranium has not been previously addressed in detail. Our analysis shows that *T. longaevus* shares many postcranial features with other tritylodontids that distinguish them from other non-mammaliaform cynodonts. The correlation between taxon size and postcranial anatomical traits is briefly explored among tritylodontids, showing that few morphological differences among species correlate with size. Analysis of the purported oldest remains of *Tritylodon*, from the Norian Los Colorados Formation of Argentina, suggests that they cannot be unambiguously assigned to this taxon, circumscribing the record of *Tritylodon* to African localities.

Key words. Postcranium. Eucynodontia. *Tritylodon longaevus*. Lower Jurassic.

Resumen. EL ESQUELETO POSTCRANEANO DE *TRITYLODON LONGAEVUS* DEL JURÁSICO INFERIOR DE ÁFRICA DEL SUR. *Tritylodon longaevus* es uno de los taxones más comúnmente representados en las faunas del Jurasico Inferior de la Cuenca del Karoo. Este taxón es únicamente conocido a través de su anatomía craneana y dentaria mientras que su esqueleto postcraneano no ha sido previamente descripto en detalle. El presente estudio muestra que *T. longaevus* comparte con otros tritilodóntidos varios rasgos postcraneanos que los diferencian de otros cinodontes no mamaliaformes. También se explora aquí la correlación entre el tamaño corporal y a las variaciones en la anatomía postcraneana observadas en los tritilodóntidos, encontrándose que sólo unas pocas diferencias morfológicas entre especies se correlacionan con el tamaño. El re-análisis de los supuestos registros más antiguos (Noriano) de *Tritylodon*, procedentes de la Formación Los Colorados de Argentina, indica que estos restos no pueden asignarse sin ambigüedades a este taxón, circunscribiendo la distribución geográfica de *Tritylodon* a localidades de África.

Palabras clave. Esqueleto postcraneano. Eucynodontia. *Tritylodon longaevus*. Jurásico Inferior.

TRITYLODONTIDS represent the last experiment in diversification among herbivorous non-mammaliaform cynodonts (Clark and Hopson, 1985; Kemp, 2005, Watabe et al., 2007). This group was exceptionally well represented in Laurasia and, although sparsely recorded, was also present in Gondwana. A possible reason for their success is their masticatory apparatus, very similar to that of allotherians and rodents, characterized by the lack of canines and the presence of two or more longitudinal rows of cusps in the postcanines (Parrington, 1981; Kemp, 2005). Tritylodontids thus represent the oldest cynodonts in which there is evidence of predominant propalinal jaw movements during chewing, although propaliny has been proposed to have been a common mechanism among toothless dicynodonts (Crompton and Hotton, 1967; Angielczyk, 2004).

Tritylodontids are remarkably diverse, with at least 20 recognized species (Tab. 1) in ~80 million years of existence (Norian to Hauterivian). Particularly well-represented in Jurassic terrestrial ecosystems, tritylodontids are known from the Lower Jurassic of South Africa and Lesotho (Owen, 1884; Broom,1910; Broili and Schröder, 1936; Ginsburg, 1962), the Upper Triassic and the Lower and Middle Jurassic of Europe, the Lower Jurassic of western North America and Antarctica, the Middle Jurassic of Mexico, the Lower to Upper Jurassic of China (Young, 1940, 1947, 1982; Kühne, 1956; Sun, 1984; Kermack, 1982; Clark and Hopson, 1985; Sun and Li, 1985; Lewis, 1986; Sues, 1986, Luo and Wu, 1994; Maisch et al., 2004; Watabe et al., 2007; Hammer and Smith, 2008), and the Lower Cretaceous of Russia and Japan (Tatarinov and Matchenko, 1999; Matsuoka and Setoguchi, 2000; Lopatin and Agadjanian, 2008; Matsuoka et al., 2016). This diversity and distribution demonstrate that these non-mammaliaform cynodonts were remarkably ubiquitous when therapsid dominance in Mesozoic ecosystems was near its end.

Considering the notable diversity of the group, it is not surprising that tritylodontids are among the non-mammaliaform cynodont groups for which a considerable amount of postcranial information is available (Tab. 1). Almost complete skeletons are known for three taxa: *Oligokyphus major* Kühne, 1956, *Bienotheroides* Young, 1982 (see Sun and Li, 1985), and *Kayentatherium wellesi* Kermack, 1982 (see Sues and Jenkins, 2006). In addition, postcranial elements of *Bienotherium yunannense* Young, 1940 (see Young, 1947), *Bienotheroides ultimus* Maisch et al., 2004, and an indeterminate tritylodontid (Sullivan et al., 2013) have also been described. The South African *Tritylodontoideus maximus* Fourie, 1962, represented by negative moulds on two rock slabs, also preserves a large portion of the skeleton, although the postcranium was never described in detail (Fourie, 1962, 1963). Postcranial elements of *Dinnebitodon amarali* Sues, 1986, from the Kayenta Formation (Early Jurassic, North America) have been reported but remain mostly undescribed (Sues, 1986; Sues and Jenkins, 2006).

Tritylodon longaevus Owen, 1884 is one of the most common members of the Lower Jurassic faunas of the Karoo Basin (Kitching and Raath, 1984; Smith and Kitching, 1997). The skull and dentition of this taxon are fairly well known (Owen, 1884; Broom, 1910; Ginsburg, 1962, Gow, 1986, 1991). On the other hand, studies considering its postcranium are purely histological in nature (De Ricqlès, 1969; Botha, 2002; Ray et al., 2004; Chinsamy and Hurum, 2006; Botha-Brink et al., 2012) except for Broili and Schröder's (1936) description of a distal portion of a humerus. Thus, the main aim of the present study is to provide a complete description of the known postcranial remains of *Tritylodon longaevus*. Additionally, possible correlations between taxon size and various postcranial anatomical features in tritylodontids will be explored in view of the recognition of different sized forms with known postcranium (Tab. 1). We also re-describe the oldest putative remains of tritylodontids, namely isolated postcranial elements from the Norian Los Colorados Formation of Argentina (Bonaparte, 1971), in order to assess their taxonomic identity.

***Institutional Abbreviations*. BP**, Evolutionary Studies Institute (formerly Bernard Price Institute for Palaeontological Research), University of the Witwatersrand, Johannesburg, South Africa; **CXPM-C**, Chuxiong Prefectural Museum, Chuxiong, China; **IVPP-V**, Institute of Vertebrate Paleontology and Paleoanthropology, Chinese Academy of Sciences, Beijing, China; **MCZ**, Museum of Comparative Zoology, Harvard University, Cambridge, U.S.A.; **PVL**, Instituto Miguel Lillo, Universidad Nacional de Tucumán, Tucumán, Argentina.

MATERIALS AND METHODS

Tritylodon is diagnosed on the basis of craniodental features whereas postcranial evidence has been neglected. Accordingly, the specimens available to us (Tab. 2) were referred to *Tritylodon* and incorporated into our study only if they either included diagnostic craniodental elements in addition to postcranial bones, or could be established as belonging to *Tritylodon* based on size, provenance and detailed morphological comparisons to specimens of both *Tritylodon* and other tritylodontids that did include diagnostic elements. Taxonomic revision of the genus *Tritylodon* is long overdue in view of the discovery of hundreds of new South African tritylodontid specimens in the last 30 years, several of which include complete skulls; however, such a revision is beyond the scope of this paper. Hence, we provisionally consider this genus monospecific and refer the studied postcranial elements to *Tritylodon longaevus*, the only tritylodontid species currently recognized in the Upper Elliot Formation.

Three of the *Tritylodon* specimens analyzed here (BP/1/4782, BP/1/5167, and BP/1/5269) are interpreted to be juveniles on the basis of craniodental features and the relatively small size as judged from the basal skull length (defined as the distance between the anteriormost tip of the snout and the posteriormost end of the occipital condyles). The descriptions of certain postcranial elements were based entirely on these juvenile specimens.

When both juvenile and adult examples of a particular element were available for description, any morphological differences between them have been highlighted.

In order to analyze possible correlations between body size and postcranial features, we estimated the body mass of the tritylodontids for which postcranial elements are known (Tab. 3). In this task, we employed equations based in modern mammals (van Valkenburgh, 1990; Anyonge, 1993) that we believe are the best proxies available. Nevertheless, the results obtained might not be completely accurate due to differences in body proportions between tritylodontids and the extant forms employed to produce the formulas. Equations that would result in estimations suitable for "all carnivores" were used for being more taxonomically (and morphologically) comprehensive than other available formulas that would apply for less inclusive groups (see Fariña et al., 1998). Although many formulas are available to estimate the body mass (Fariña et al., 1998), we preferred an equation (1) based on skull length (van Valkenburgh, 1990) considering that it is available for most of the taxa surveyed. Otherwise, femur and humerus length (Anyonge, 1993) based formulas (2, 3) were employed.

(1) Log (body mass) = 3.13log(skull length in millimetres) – 5.59

(2) Log (body mass) = 2.92log(femur length in millimetres) – 5.27

(3) Log (body mass) = 2.93log(humerus length in millimetres) – 5.11

DESCRIPTION

Axial Skeleton

The description of the axial skeleton of *Tritylodon* is based on specimens BP/1/4782, BP/1/4785, BP/1/4965, BP/1/5089, and BP/1/5167. In some cases, specimens were labeled with a lower case letter following the collection number in order to identify isolated and groups of associated or articulated vertebrae that belong to the same specimen. Most of these lower case letters were assigned previous to our analysis of *Tritylodon* specimens thus the alphabetical order does not necessarily correlates with the inferred vertebral order. In addition, the letters are not always correlative and not all the letters have been employed to label the vertebral elements (Tab. 4).

Atlas-axis. The atlas-axis centrum is present in two juvenile individuals of *Tritylodon*, namely BP/1/4782 and BP/1/5167 (Fig. 1), and in the adult BP/1/4965 (Fig. 2). The atlanto-axial centrum is almost complete with only part of the neural spine missing in BP/1/4782 (Fig. 1.3–4, 7–8, 11–12), whereas most of the neural spine is lacking, the centrum is broken, and clear signs of distortion are observed in BP/1/5167 (Fig. 1.1–2, 5–6, 9–10). The atlas-axis centrum is complete but only can be observed ventrally in BP/1/4965 (Fig. 2). There is no record of the atlas neural arch or intercentrum.

Prezygapophyses are absent whereas postzygapophyses are relatively well developed with the postzygapophysal facets oriented latero-ventrally (Fig 1.5–8). The dorsal margin of the incomplete neural spine of BP/1/4782 suggests that the missing dorsal portion of the spine was very thin. The transverse processes, completely preserved in BP/1/5167, show straight anterior and posterior margins and are directed laterally, posteriorly and ventrally (Fig. 1.5–6, 9–10). The distal end of the processes is flattened and slightly concave. The orientation of the transverse process is different on the two sides of the specimen BP/1/5167 due to deformation. In BP/1/4782, what is preserved of the transverse processes points to a posteroventral orientation (Fig. 1.7–8, 11–12), suggesting that the left transverse process in BP/1/5167 is likely to be closer to its original orientation. The dorsoventrally compressed centrum is ellipsoid in posterior view and has an anteroposterior length of 14.8 mm in BP/1/4782, 17.9 mm in BP/1/5167, and 22.1 mm in BP/1/4965 (Tab. 5), although it has to be considered that the atlas-axis centrum of BP/1/5167 is visibly deformed. The dens is notably distinct from the centrum, forming a hemispheric surface encircled laterally and ventrally by well-developed convex articulation facets for the atlantal arches and atlas intercentrum (Fig 1). The dens is even more distinct in the adult BP/1/4965 (Fig. 2). The dorsal surface of the dens is horizontal and appears as a flat facet. In ventral view, the centrum has an isosceles trapezoid outline with the anterior margin, limited by the ventral border of the articulation facets, clearly more expanded laterally than the posterior one in the juvenile specimens (Fig. 1.9–12). On the other hand, the atlas-axis centrum of the adult specimen is approximately rectangular in ventral aspect (Fig. 2). A noteworthy feature in the middle portion of the ventral face of the centrum is a pair of rounded tubercles, interpreted as parapophyses, which extend onto the lateral surface of the centrum (Fig. 1.5–12). It is possible to observe a rib articulating with the parapophysis of this vertebra in the adult specimen. In BP/1/4965, a strong crest, transverse to the long axis of the centrum and connecting the parapophyses, is interpreted as the boundary between the atlantal and axial centra. The suture between atlantal and axial centra is hinted in the juvenile specimens by a weakly developed crest in BP/1/5167 (Fig. 1.9–10) and a broad blunt crest in BP/1/4782 (Fig. 1.11–12). Unlike BP/1/4965, the centrum is constricted behind the parapophyses in BP/1/4782 and BP/1/5167 (Fig. 1.9–12). A well developed mid-ventral keel is present on the ventral surface of the atlas-axis centrum in BP/1/4965. This keel is limited to the posterior (i.e., axial) portion of the centrum, behind the parapophyses in BP/1/4782 (Fig. 1.11–12) whereas in BP/1/5167 it continues anteriorly (i.e., onto the atlantal centrum) but without reaching the margin of the facet for the atlantal intercentrum (Fig. 1.9–10).

Postaxial cervical vertebrae. The first four articulated postaxial cervical vertebrae (c3-6) are present and articulated in BP/1/4965, although only poorly exposed (Fig. 2). Additionally, a series of five cervical vertebrae from the juvenile specimen (BP/1/4785), preserved in two separate articulated sets (BP/1/4785a and b), are interpreted as the first 5 postaxial vertebrae (c3-4 in BP/1/4785a and c5-7 in BP/1/4785b; Fig. 3.1–6, 9–10, 13–18). Although the continuity between these sets is not certain, we assume that there are no missing elements based on the regularly increasing anteroposterior length of these centra (Tab. 5). The observable features of the articulated cervical vertebrae (c3-c5) of the adult specimen BP/1/4965 agree with those seen in the putatively corresponding cervicals of BP/1/4785, supporting the vertebral number identifications postulated for the latter specimen.

The cervical centra are platycoelous and rectangular in ventral view (Fig. 3.3–4). In BP/1/4965, until the sixth vertebra, the centra bear a keel and are rectangular (Fig. 2; Tab. 5), with a posteriorly decreasing the length to width ratio. On the other hand, in BP/1/4785, the third and fourth vertebrae are remarkably wider than long (length/width ratio is 0.58 and 0.59, respectively) (Fig. 3.3–4; Tab 5) whereas in more posterior cervicals (c5 to c7) the length to width ratio is higher (0.68, 0.68, and 0.79, respectively) (Fig. 3.9–10; Tab. 5). The centra of the three anteriormost vertebrae are wider than tall, with an oval to triangular shape in anterior or posterior view (Fig. 3.5–6). On the other hand, the centrum of the last preserved cervical vertebra (c7) is less dorsoventrally compressed in posterior aspect. Although broken in the first postaxial cervical vertebra (c3), well developed parapophyses on the ventroanterior portions of the centra of the three anteriormost cervical vertebrae (c3 to c5) project ventrolaterally (Fig. 3.3–4, 9–10, 15–18). In c6 and c7, the reduced parapophyses are displaced dorsally, lying on the anterior rims of the centra in lateral view (Fig. 3.15–18). There is a low mid-ventral keel in c3 and c4 (Fig. 3.3–4). In c5, the ventral surface of the centrum is flat and broad whereas in c6 and c7 this surface is spool-shaped (Fig. 3.9–10). The transverse process is almost at the level of the posterior margin of the centrum in c3, but it is slightly displaced anteriorly in c4, although still at the same level relative to the postzygapophyses as in c3 (Fig 3.1–4). The transverse process becomes progressively more anterior in the subsequent cervical vertebrae, and approaches the anterior margin of the centrum in c7 (Fig. 3.9–10, 13–18). These processes are incompletely preserved in all the cervical vertebrae, but it can be ascertained that they were mainly laterally directed. The transverse process is compressed anteroposteriorly in c3, but dorsoventrally flat in c4 (Fig. 3.1–2). On the other hand, the transverse processes of c5 to c7 are cylindrical and become more robust posteriorly (Fig. 3.15–18). The prezygapophyses are missing in c3 and c5. In c4, they project anteriorly to the level of the transverse process of the preceeding vertebra, whereas in c6 and c7 they are much shorter, only reaching the posterior margin of the centrum of the preceding vertebra (Fig. 3.1–2, 15–18). In c3-c4, the postzygapophyses extend beyond the neural spine and bear flat, oval articular surfaces inclined approximately 30º to the horizontal plane. In c6, the postzygapophyses do not projected so far posteriorly beyond the neural spine. Moreover, they are much more vertical (about 70º to the horizontal plane) and the notch separating them from the centrum is broader than in c3 and c4. The zygapophyses become progressively closer to the sagittal plane posteriorly. The distance between the prezygapophyses, measured between the external margins of the left and right prezygapophyseal articular surfaces, is almost the same in c4 and c7 (approximately 13 mm to 13.5 mm apart). The neural arch and part of the dorsoposteriorly directed neural spine (4.7 mm tall) are preserved in c6 (Fig. 3.15–18).

BP/1/4782b is a very small (Tab. 5), partially preserved cervical vertebra missing most of the neural arch. It is interpreted as a c4 by comparison to specimen BP/1/4785 due to the presence of: mid-ventral keel; robust, anteroventral parapophyses that project ventrolaterally; and transverse process only slightly displaced anteriorly from the posterior margin of the centrum.

A postaxial cervical vertebra interpreted as c4 is the smallest element in specimen BP/1/5167x (Fig 3.7–8, 11–12). The platycoelus centrum is very compressed anteroposteriorly and broad laterally (Tab. 5). There is a very prominent mid-ventral keel, which is much better developed than in any other of the cervical vertebrae available. The parapophyses are anteroventrally placed, project lateroventrally and slightly posteriorly, and are less robust than in BP/1/4785. The transverse processes are slightly more anteriorly placed than in the c4 of BP/1/4785. They are directed laterally and slightly ventrally, and situated approximately at the mid-length of the vertebra in lateral view, roughly beneath the postzygapophyses (Fig. 3. 7–8, 11–12). The diapophyseal facets are at the tips of the transverse processes, and face mainly laterally but also posteriorly and ventrally. The neural arch is inclined anteriorly, so that the prezygapophyses extend beyond the anterior border of the centrum whereas the postzygapophyses do not reach the posterior one. The pre- and postzygapophyses are at the same distance from the sagittal plane and well set apart (12.7 mm, measured between the external margins of the left and right zygapophyseal articular surfaces), approximately above the lateral margins of the centrum in anterior/posterior view. The zygapophyses are inclined about 30º - 40º from the horizontal (Fig. 3.7–8, 11–12). The articular surfaces of the postzygapophyses are flat, but the articular surfaces of the prezygapophyses are obscured by matrix. The neural spine is relatively short and slightly dorsally directed. The neural canal is large (7.45 mm wide; approximately 69% of the width of the centrum) (Fig. 3.11–12).

***Dorsal vertebrae*.** Ten vertebrae from specimen BP/1/4785 (designated as BP/1/4785c, d, e, f, g, h, i, and j) are identified as dorsals (see Tab. 4–5). Although the exact position of each of these vertebrae cannot be unambiguously ascertained, a relative order is suggested mainly on the basis of the vertebral body size (but see below for exceptions). Thus, for the sake of simplicity and easy reference, the dorsal vertebrae will be referred to as dx1 to dx8 from the most anterior to the last posterior one. The three remaining dorsal elements of BP/1/4785 (g, h, i) seem to represent more posterior vertebrae than dx9-11; thus we refrained to assign them a vertebral number. As that of BP/1/4785 is the most complete set of dorsal vertebrae recorded for a *Tritylodon* specimen, we will use it as a reference to suggest the relative position of the dorsal vertebrae of other specimens.

BP/1/4785c and d are identified as dx1 and dx2, respectively, because these vertebrae are similar enough in size and morphology to the last cervical (c7) to suggest that they might be the first two dorsals (Fig. 4.1–8; Tab. 5). The vertebral centra of dx1 and dx2 are spool-shaped as in c7, but the anterior and posterior margins of the body are more protrusive ventrally and the central portion of the ventral surface is flatter. Unlike in the cervicals, the transverse processes are dorsoposteriorly oriented in dx1 and the centra of dx1 and dx2 appear heart shaped, with a somewhat acute ventral apex, in anterior view (Fig. 4.1–8). The vertebra dx1 differs from the c6 in having a more posteriorly placed neural spine (the posterior part of the neural arch is not preserved in c7 and dx2) which is also not laminar as in c6 but more robust and triangular in cross-section.

BP/1/4785e includes two articulated vertebrae, namely dx3 and dx4 (Fig. 4.9–12). Although they are relatively similar in size to dx2, the possibility of one or more missing vertebrae between dx2 and dx3 cannot be disregarded. The relatively large size difference between the articulated dx3 and dx4 when compared to that between dx1 and dx2 is striking. Vertebrae dx3 and dx4 are extremely similar to the slightly larger dx5 (BP/1/4785f; Fig. 4.13–16). The only noteworthy difference between these vertebrae involves the progressively larger distance between the transverse process and the prezygapophysis (Fig. 4.9–16), a transformation probably linked with the increasingly posterior position of the transverse processes. The centrum of dx5 also differs from those of the more anterior vertebrae in being anteroposteriorly longer than laterally broad.

Vertebrae dx3-5 have the same general centrum shape as the more anterior dorsals. Unlike dx1 and dx2, however, dx3-5 share with more posterior dorsal vertebrae the presence of a crest connecting the parapophysis with the transverse processes (Fig. 4.13–16). Unlike those of c7 and dx1, the transverse processes of dx3-5 are not placed at the level of the anterior margin of the vertebral centrum; they are slightly posteriorly displaced in dx3 and approximately at the centrum mid-length in dx4 and dx5 (Fig. 4.9–16). Although only partially preserved, the transverse processes of dx3-5 are oriented slightly dorsoposteriorly, like those of dx1. The neural spine of dx3 is posteriorly inclined, at about 35º to the horizontal plane (Fig. 4.9–12). Although only the basal parts of the neural spines of dx4 and dx5 are preserved, the intact spines were probably similar to that of dx3. The neural spine orientation of dx1 and dx2 cannot be ascertained. Near the base, the neural spines of dx1 and dx3-5 are relatively robust and triangular in cross-section. The prezygapophyses of dx4 and dx5 do not extend anteriorly much beyond the anterior margin of the centrum (Fig. 4.9–14) differing from the highly protruding prezygapophysis of c7 (Fig. 3.15–18). Vertebrae dx1-3 were probably similar in this respect to the more posterior dorsals, but the prezygapophyses are broken.

There are three vertebra identified as anterior dorsal vertebrae in the juvenile specimen BP/1/5167: the isolated vertebrae BP/1/5167b and BP/1/5167z, and the smallest vertebra in the block BP/1/5167d, which also includes a more posterior dorsal vertebra (see below; Tab. 4). The anterior dorsal BP/1/5167b (Fig. 4.17–22) and the one in the block BP/1/5167d are similar to dx1-4 in BP/1/4785, BP/1/5167b being posterior to the anterior dorsal of BP/1/5167d in the vertebral series. Unlike in dx1-4 of BP/1/4785, the ventral surface of the centrum in the purported anterior dorsal vertebrae BP/1/5167b and d is not flat but acutely convex, and bears a minute mid-ventral keel. The right transverse process of BP/1/5167b is preserved partially overlapped by a misplaced rib fragment on its posterior surface and not completely free from matrix. It is large, dorsoventrally deep, and anteroventrally oriented, differing from the comparatively small, dorsoposteriorly oriented transverse process of anterior dorsals in BP/1/4785. The juvenile vertebra BP/1/5167z is also identified as a relatively anterior dorsal, but its incomplete preservation makes proper comparisons difficult. The presence of a crest between the parapophyses and the transverse process suggest that this vertebra was situated more posteriorly than BP/1/5167b and the anterior dorsal of BP/1/5167d. Comparisons to BP/1/4785 indicate that BP/1/5167z is most similar to the vertebrae identified as dx3 and dx4 (BP/1/4785e), but with the transverse process slightly more anteriorly placed.

BP/1/4782d is a fragmentary dorsal vertebra, comprising only the centrum and the incomplete right transverse process, which is most similar to BP/1/4785f (Fig. 4.13–16). However, the centrum of BP/1/4782d is more markedly spool-shaped and more slender (although this latter difference might be due to incomplete preservation of the anterior portion of the centrum).

Three closely associated vertebrae (dx6-8) in the block BP/1/4785j (Fig. 4.23–24) are interpreted to follow each other in series; however, the size differences between them seem very large for contiguous vertebrae. Vertebra dx6 is the best preserved in this group, although the prezygapophyses are missing. Similar to dx5, the width of the vertebral body is 94% of its length (Tab. 5). Unlike in more anterior dorsal vertebrae, the neural spine in dx6 is less posteriorly inclined (approximately 50º from the horizontal) and laterally compressed (Fig. 4.23–24). In dx6, the tip of the neural spine is expanded anteroposteriorly in lateral view. Due to lack of preparation and incomplete preservation, only the vertebral centra of dx7 and dx8 are available for analysis. Vertebra dx7 has a more slender centrum (width representing 90% of the length) than dx6. Unlike those of more anterior dorsal vertebrae, the vertebral body of dx8 is not spool–shaped, lacking ventrally expanded anterior and posterior margins. In ventral view, the posterior portion of the centrum is expanded laterally (Fig. 4.23–24). Additionally, the vertebral body is dorsoventrally compressed in dx8, as can be observed in posterior view.

BP/1/4785h and i are two fully prepared, isolated vertebrae (Fig. 4.25–32) that are morphologically similar to, and were found in association with, the other dorsal vertebrae of BP/1/4785; thus, we consider them as part of the same individual. However, it is puzzling that BP/1/4785h and i are unusually large when compared to the more anterior vertebrae (Tab. 5), BP/1/4785h being slightly larger than BP/1/4785i (compare Figure 4.25–28 with Figure 4.29–32). BP/1/4785h and i are interpreted here as consecutive vertebra that do not immediately follow dx8 (i.e., they are more posterior than dx9-10) but it is not possible at present to determine more accurately their vertebral number. As in more anterior dorsals (except dx8), BP/1/4785h and i have spool-shaped centra, although the anterior and posterior rims of the body are more robust and less ventrally prominent. The centrum of BP/1/4785h is slender (width is approximately 80% of the anteroposterior length) whereas that of BP/1/4785i is stouter (width is approximately 90% of the anteroposterior length). As in dx6, the neural spines of BP/1/4785h and i are flat laterally. On the other hand, the neural spines of BP/1/4785h and i, although broken near the base, are interpreted as almost vertical, unlike those of more anterior dorsals. The prezygapophyseal facets of BP/1/4785h, as well as those of the more anterior dorsal vertebrae, are at the end of well-defined dorsoanteriorly directed processes (Fig. 4.25–28). However, in BP/1/4785h the prezygapophyses are more anteriorly positioned, protruding well beyond the anterior margin of the centrum. The pre- and postzygapophyseal facets are inclined at approximately 70° to the horizontal in BP/1/4785h, whereas the corresponding angle is approximately 30º-35º in dx4. BP/1/4785i is considered here to be more posterior than BP/1/4785h mainly due to characteristics of its prezygapophyses. Unlike other dorsal vertebrae, the prezygapophyses of BP/1/4785i are very short. They do not extend beyond the anterior end of the vertebral body, and the posterior portion of the articular surface of each prezygapophysis is at the level of the transverse processes (Fig. 4.29–32). Unlike in BP/1/4785h and more anterior dorsal vertebrae, the articular facets of the zygapophyses of BP/1/4785i form an approximately 15º-20º angle to the horizontal. The postzygapophyseal facets of BP/1/4785i are positioned beyond the posterior margin of the vertebral body (Fig. 4.29–32) whereas they are more anteriorly placed in more anterior dorsal vertebrae (Fig. 4.25–28). Additionally, the neural spine in BP/1/4785i is posteriorly positioned, exceeding the vertebral body, when compared to more anterior dorsals.

Two additional specimens (BP/1/4782c and BP/1/5089) include vertebral elements that are interpreted to represent a position between BP/1/4785h and i. The centrum width to length ratio of BP/1/4782c (85%) is intermediate between those of BP/1/4785h and i. Unlike in these specimens, the centrum of BP/1/4782c is not markedly spool-shaped (the anterior and posterior portions of the body are not so ventrally expanded relative to the central portion) and has a mid-ventral keel. Additional differences are the great robustness and more posterior placement of the transverse processes, the slight posterior inclination of the neural spine, and the inclination of the postzygapophyses at approximately 45º from the horizontal. The body of dorsal vertebra BP/1/5089 is most comparable to that of BP/1/4785h, whereas the neural arch, prezygapophysis, and neural spine resemble those of BP/1/4785i.

In addition to the cervical element described above, BP/1/5167x also includes a more posterior dorsal element (Fig. 3.7–8, 11–12). The centrum of the dorsal vertebra of BP/1/5167x differs from that of BP/1/4782c only in being more markedly spool-shaped. The fact that this element is intermediate between BP/1/4785h and BP/1/4782c with respect to zygapophysis and neural spine morphology suggests that BP/1/5167x represents a correspondingly intermediate vertebral locus.

The larger element in BP/1/5167d is a dorsal vertebra probably anterior to BP/1/5167x and almost identical to BP/1/4785h. The only noteworthy differences are that in the large dorsal of BP/1/5167d the centrum is stouter (85% width/length ratio, in comparison to 80% in BP/1/4785h; Tab. 5), the anterior and posterior portions of the centrum are less robust, and the postzygapophysis is oriented at a low angle to the horizontal (approximately 35º: similar to BP/1/5167d, but not to BP/1/4785h, in which the angle is 70º).

BP/1/5167e is a distorted dorsal vertebra almost identical to that of BP/1/5167x. The only clear difference is that in BP/1/5167e the postzygapophyseal facet forms a slightly lower angle to the horizontal (approximately 25º-30º) than in BP/1/5167x, suggesting that the former might be interpreted as a more posterior dorsal.

BP/1/4785g is an isolated element that represents the most posterior dorsal vertebra preserved in the specimen. This vertebra is similar to what Kühne (1956) interpreted as the dorsal 16 of *Oligokyphus* (see comparisons below). The centrum is dorsoventrally compressed, with a rather flat ventral surface. It is not spool-shaped; however, the anterior portion of the centrum is more expanded laterally than the posterior one, whereas the central portion appears constricted in ventral view. Strong crests connect the transverse processes to the parapophyses within the anterior portion of the centrum. Unlike in more anterior dorsal vertebrae, the neural arch is very low and the transverse processes are laterally and slightly anteriorly oriented. The prezygapophyseal facets are almost horizontal and positioned just anterior to the bases of the transverse processes on the neural arch, lacking anteriorly projecting prezygapophyseal processes (Fig. 4.33–34). Although not preserved, the postzygapophyses and neural spine must have projected posteriorly beyond the vertebral centrum.

***Caudal vertebrae*.** Two vertebral centra of different sizes, belonging to specimen BP/1/5089, are identified as caudal vertebrae (Tab. 4–5). They are spool-shaped, very elongated, and platycoelous (Fig. 5). The neural arch is missing but it extended along almost the entire length of each centrum (Fig. 5.5–6, 11–12), unlike in the cervical and dorsal elements.

Pectoral girdle

Scapula**.** The scapula of *Tritylodon* is known from several specimens, of which the right scapula of BP/1/5167 is the best preserved (Fig. 6.1–4). The scapula is slightly bowed laterally, although in some specimens it has been flattened by deformation (e.g., BP/1/5167). The blade is triangular, being expanded dorsally and narrow ventrally (Fig. 6.1–4). The medial surface of the scapular blade is flat, but its anterior and posterior borders are reflected, delimiting a well defined triangular infraspinous fossa (Fig.6.1–2). The posterior border is laminar lacking an expanded area for the origin of the *caput scapularis* of the *M. triceps brachii* (Jenkins, 1971; Sues and Jenkins, 2006). The anterior border or scapular spine is thicker than the posterior one, and thickens further as it continues ventrally towards the acromion (Fig.6.1–2). The spine ends in a short acromial process directed anteriorly with the tip slightly upturned dorsally. The incipient supraspinous fossa is almost excluded from the lateral view and only represented by a slightly concave surface anterior to the scapular spine (Fig.6.1–2). There is no clearly defined clavicular facet, and the clavicle might have contacted the flat ventromedial surface of the acromion. The dorsal margin of the scapula is rounded anteriorly and posteriorly in lateral view (Fig.6.1–2). The central part of the margin is almost laminar, but the dorsal margin thickens slightly posteriorly and becomes very robust and triangular in cross-section anteriorly, where it merges with the scapular spine. A shallow concave postscapular fossa, facing mostly posteriorly and slightly medially, is present along the whole posterior surface of the scapula. This was interpreted as the origin area for the *M. teres major* (Gregory and Camp, 1918; Jenkins, 1971; Sues and Jenkins, 1986). The base of the bone is separated from the scapular blade by a constriction ventral to the acromial process (Fig. 6.1–4). The slightly concave oval glenoid facet is oriented ventrally and bordered by a thick rim. Anterodorsal to the glenoid facet, the base of the scapula forms a triangular flange-like projection (Fig. 6.1–4), probably for insertion of the *M. supracoraoideus* (see Jenkins, 1971).

Coracoid. The complete left coracoid and partial right coracoid are known in specimen BP/1/5167 (Fig 6.5–16). The coracoid is very small in comparison to the scapula. Anteriorly, the coracoid contacts a thin strip of bone corresponding to the posteroventralmost portion of the procoracoid; however, coracoid-procoracoid suture is not readily recognizable. The glenoid facet is narrow, elongated, oval in outline, and oriented posterodorsally (Fig. 6.9–10, 15–16). Medially adjacent to the glenoid facet, the anterodorsal portion of the coracoid is very robust and bears a facet for the contact with the scapula (Fig. 6.7–10, 15–16). The procoracoid is excluded from the glenoid cavity. The coracoid is high dorsoanteriorly but tapers posteriorly, ending in a slightly rounded area that represents the tuberosity for the coracoid head of the triceps (Fig. 6.11–14). This tuberosity, representing the posterodorsal corner of the coracoid, is continuous with the thin laminar posterior margin of the bone. This posterior portion of the coracoid is comparatively higher than in other non-mammaliform cynodonts, including *Kayentatherium* (Jenkins, 1971; Sues and Jenkins, 2006). The continuous shallowly concave lateral surface of the coracoid represents the fossa for the *M. coracobrachialis*. The medial face of the coracoid is flat except that the anterior area ventral to the facet for the scapula, close to the inferred suture with the procoracoid, is relatively depressed. This area has been associated in other non-mammaliaform cynodonts (Jenkins, 1971) with the insertion of the sterno-costo-coracoid musculature.

Procoracoid. The partial right and left procoracoids of BP/1/5167 are preserved, and are firmly sutured to their respective coracoids (Fig. 6.5–14). Only a tiny portion of the left procoracoid is present, whereas the right one is complete. The procoracoid is laminar and rectangular, tapers slightly posteriorly, and does not contribute to the glenoid. The procoracoid foramen is close to the anterodorsal margin of the lateral surface of the procoracoid (Fig. 6.5–8, 11–12). The lateral surface is depressed just above the procoracoid foramen margin, so that the foramen opens into a groove dorsally. The medial opening of the procoracoid foramen is on the inferred suture between the procoracoid and the coracoid. A groove extends across the medial surface from the posteroventral corner of the procoracoid to the procoracoid foramen.

Forelimb

***Humerus*.** Several humeri have been recovered, complete or partially preserved: BP/1/4785, BP/1/5089, and BP/1/5671. The humerus is relatively robust, with expanded proximal and distal portions and a short diaphysis (Tab. 6). The diaphysis, measuring from the distal inflexion of the deltopectoral crest to the proximal rim of the entepicondylar foramen, is only 10% of the total length of the bone in BP/1/5671 and 17% in BP/1/4785. The humerus is more expanded distally than proximally, although the amounts of both proximal and distal expansion differ between the two complete humeri in the sample. The maximum width across the epicondyles is 48% of the humeral length in the larger specimen (BP/1/5671) and 51% in the smaller one (BP/1/4785). The maximum width of the humerus at the proximal region is 40% and 34% of the length of the bone in the larger and smaller specimens, respectively. The proximal and distal regions of the humerus are rotated relatively to each other about the humeral long axis at an angle of approximately 40º in BP/1/5671 compared to only 30º in BP/1/4785; however, this difference might be due to post-mortem deformation.

The humeral head is oval and directed dorsolaterally (Fig. 7.3–6). It projects above the surface of the shaft and is demarcated distally by a thin ridge. Proximally, the articular surface of the humeral head continues medially but not laterally. Distinct greater and lesser tuberosities are lacking. The proximomedial corner of the humerus, where the lesser tuberosity would be expected, is robust and, being continuous with the humeral head and forming part of the proximal surface of the bone, might have been covered with cartilage. Laterally, the proximal surface of the humerus is continuous with the robust deltopectoral crest (Fig. 7.1–2, 5–6). Ventrally, the proximal surface ends sharply with the beginning of a relatively shallow bicipital groove that is limited by a low and broad ridge medially and the protruding deltopectoral crest laterally (Fig. 7.1–2). The deltopectoral crest extends for approximately half the length of the humerus and forms an angle of about 100º with the lateromedial axis of the proximal portion of the bone. The deltopectoral crest continues distomedially towards the entepicondyle as a low ridge that forms the medial boundary of the entepicondylar foramen (Fig. 7.1–2). A shallow depression is present on the lateral surface of the deltopectoral crest. This surface is limited medially by a low crest that runs from the ectepicondyle to the humeral head. This fossa has been interpreted as the origin of the *M. brachialis*, whereas the low crest would represent the insertion for the *M. teres minor* (Jenkins, 1971). Medial to the purported crest for the *M. teres minor*, another crest extends across the dorsal surface of the humerus from the medial portion of the humeral head to a tuberosity on the medial margin of the bone. This tuberosity occupies a similar position to the groove described by Jenkins (1971), which he interpreted as the place of insertion of the *M. teres major* and/or the origin of one of the *humeral triceps* heads.

The distal portion of the humerus is triangular in outline (Fig. 7.1–4). The entepicondyle is more robust, and projects slightly further from the midline of the humerus, than the ectepicondyle. The latter continues proximally as a flange-like structure. In the largest humerus available (BP/1/5671), the ectepicondylar flange bears on its ventral surface a small groove that defines a proximolaterally positioned, somewhat inflated area that may be associated with muscular attachment. The entepicondylar foramen is a short canal that trends laterally as it penetrates from the dorsal side of the humerus to the ventral side (Fig. 7.1–4, 7–8). It opens ventrally in a relatively narrow, deep depression that is medial to the ulnar condyle and does not reach the distal margin of the humerus. There is no ectepicondylar foramen.

Both the ulnar condyle and the capitulum are well developed, although the capitulum is more bulbous and larger (Fig. 7.1–2, 5–6). Dorsally, the capitulum is reduced and crest-like whereas the ulnar condyle is rounded. The capitulum projects further distally than the ulnar condyle. The capitulum and ulnar condyle wrap around the distal surface of the humerus and are clearly separated from the ent- and ectepicondyles by well defined constrictions (Fig. 7.3–4). A shallow olecranon fossa is present dorsally, and broad grooves separate the ent- and ectepicondyles from the ulnar condyle and capitulum. Ventrally, a triangular fossa is present proximal to the capitulum.

Ulna. Only the proximal portion of a left ulna has been recovered (BP/1/4785). This bone is mediolaterally flat with a hook-shaped olecranon (Fig. 8.1–6). The facet for the ulnar condyle of the humerus appears narrow and aligned with the long axis of the bone in anterior view (Fig. 8.5–6). The facet is rimmed by a low but well defined crest, and is concave lateromedially. This facet appears “C” shaped in lateral aspect, and its distal portion is anteriorly prominent relative to the ulnar shaft (Fig. 8.1–2). Lateral to the facet for the ulnar condyle of the humerus is situated a lateroanteriorly facing triangular surface, interpreted as a poorly defined facet for the radial condyle (Fig. 8.1–2). Distal to this latter facet, a similarly sized concave, triangular radial notch (*incisura radialis*) for the proximal portion of the radius (Fig. 8.1–2) is visible in lateral view. A depressed area is present on the lateral surface of olecranon, and continues as a teardrop-shaped concavity just posterior to the facet for the radial condyle. This area is interpreted as for the origin of the extensor musculature, possibly the *M. extensor carpi ulnaris* (see Jenkins, 1971). A concave area, deeper than the lateral depressed area, is present on the medial surface of the olecranon and might be associated with the origin of deep flexor musculature (see Jenkins, 1971; Fig. 8.3–4). Distal to the facet for the ulnar condyle, a small groove on the medial edge of the ulnar shaft is visible in anterior view (Fig. 8.5–6). Sues and Jenkins (2006) interpreted a similar groove as the insertion of the *M*. *brachialis* in *Kayentatherium*. The posterior surface of the olecranon is mediolaterally wide, but tapers distally into the flange-like posterior edge of the ulnar diaphysis.

***Radius*.** The left radius of BP/1/5167 was recovered, with the distal portion missing (Fig. 9), but has been sectioned for histological studies so that only a plaster cast is available. The radius is slightly bowed posteriorly and laterally. The proximal surface of the radius is oval, concave, and rimmed by a bulbous lip (Fig. 9). A slightly more thickened portion of this rim might represent the facet for the contact with the ulna (Fig. 9.5–6). The proximal surface of the radius is inclined medially and slightly anteriorly. A distinct crest for the radioulnar interosseous ligament extends from the proximal rim anterior to the facet for the ulna (Fig. 9.5–6). This crest becomes more robust and curves anteriorly as it extends distally, forming a bicipital tuberosity that represents the point of attachment for *M*. *biceps brachii*.

***Carpus and manus*.** A series of bones from the manus are preserved in contact with the left zygoma and orbit of BP/1/4976. A large bone interpreted as the radiale is exposed in dorsal view next to a smaller triangular element identified here as the lateral centrale (Fig. 10.1–2). The radiale is a rectangular bone, slightly longer proximodistally than broad lateromedially. Laterally, there is a round depression, presumably for contact with the lateral centrale. This lateral notch is rimmed medially by a bulbous lip. The medial margin of the dorsal surface of the radiale also forms an inflated lip. The medial and lateral lips define a central groove on the dorsal surface of the bone (Fig. 10.1–2). The lateral surface of the radiale is flat, and dorsoventrally higher than the slightly convex distal surface. Additionally, ten disarticulated long bones of the manus are preserved. The one closest to the radiale (Fig. 10.1–2) is the most robust and is interpreted as a metacarpal. Two other bones are similar in length (2.1mm), but remarkably thinner. The remaining elements seem to be shorter, as well as thin.

An isolated phalange from specimen BP/1/5167 has been recovered (Fig. 10.3–10). The generalized features of this element make it impossible to ascertain if it belongs to the pes or the manus. Thus, we arbitrarily describe the recovered phalange in this section. It is a slender, dorsoventrally compressed element that appears lateromedially symmetrical in dorsal or ventral view (Fig 10.7–10), smaller than the bones of BP/1/4976. The proximal surface is shallowly concave, and inclined to face slightly dorsally. Two distal condyles, one slightly better developed than the other, define a shallow pulley. The distal articular surface is directed mainly ventrally and anteriorly. Lateral and medial collateral ligament pits are present (Fig. 10.3–6).

Pelvic girdle

Ischium. The right ischium of BP/1/5269 is nearly completely preserved, although it is partially obscured in lateral view by a superposed indeterminate fragmentary bone (probably a fragment of illiac blade). An acetabular portion, a neck, and an ischial plate are recognizable (Fig. 11.17–18). The facet for articulation with the ilium is not clearly observable due to breakage, but was probably anterior in position. The acetabular facet is concave, anterolaterally oriented, and rimmed by a low supraacetabular crest in its dorsal half (Fig. 11.15–16). The facet for the pubis is obscured by matrix but probably faces ventrally.

The neck of the ischium is not strongly constricted, being dorsoventrally high and anteroposteriorly short (Fig. 11.17–18). Dorsally, the neck of the ischium lacks a groove and is smoothly convex. The dorsal surface of the ischium is broad and does not taper posteriorly in dorsal view.

The triangular ischial plate has a robust dorsal portion, but is thin ventrally. The dorsally directed posterodorsal corner of the ischial plate represents a poorly developed ischial tuberosity (Fig. 11.17–18). Although the anterior margin of the ischial plate’s ventral portion is not perfectly preserved, it can be ascertained that this plate was broad anteroposteriorly and that the obturator foramen was relatively small. The ischial plate is slightly concave medially and flat to somewhat convex laterally.

Hindlimb

Femur. The femur is only known from its proximal and distal portions (BP/1/4783, BP/1/5089, BP /1/5152a, BP/1/5167, BP/1/5305, BP/1/5516, and BP/1/5671). The femoral head is almost hemispherical, and projects dorsomedially as well as proximally (Fig. 11.1–8). A well developed femoral neck is lacking, although the rugose articular surface of the femoral head is limited distally by a constricted area that separates the head from the expanded triangular proximal portion of the femur in dorsal view (Fig. 11.1–2). Ventrally, the well defined but not very extensive intertrochanteric fossa is located distal to the femoral head and between the trochanters (Fig. 11.5–6). Distal to the intertrochanteric fossa, the ventral surface of the proximal portion of the femur is flat to slightly convex, lacking a fossa for the adductor musculature like that described by Jenkins (1971). The trochanters are in a ventral position relative to the femoral shaft (Fig. 11.3–4, 7–8), separated from the femoral head by broad notches, and situated approximately in the lateromedial plane. In the largest specimens, the trochanters are notably massive and robust. The greater trochanter is directed proximally to proximolaterally and the lesser trochanter proximomedially. The lesser trochanter is distal to the greater one, and also lies closer to the femoral head given the medial curvature of the latter. The greater trochanter is more robust, and flares more strongly from the central axis of the shaft, than the lesser one (Fig. 11.1–2, 5–6). The shaft is oval in cross-section, being more compressed dorsoventrally than lateromedially.

Only poorly preserved distal portions of the femur have been recovered. In ventral view, the lateral and medial condyles are both well developed ventrally, the medial one being larger. However, the condyles neither protrude distally nor continue onto the dorsal surface of the femur. A deep intercondylar fossa is present between the condyles ventrally.

Tibia. A poorly preserved, incomplete ?right tibia of BP/1/5089 is represented by part of the diaphysis and the distal portion (Fig. 11.9–12). This bone is strongly crushed, obscuring any morphological features that might be of interest. The surface we interpret as the medial side of the bone is convex, whereas the lateral side is flat probably as consequence of deformation. The distal portion projects more strongly posteriorly than anteriorly (Fig. 11.9–12).

Fibula. The poorly preserved right fibula of specimen BP/1/5089 has been recovered (Fig. 11.13–14). The bone is missing its proximal and distal portions, and is still covered with matrix posteriorly. In anterior aspect, the fibula is slightly curved laterally and relatively expanded proximally, but tapers distally (Fig. 11.13–14). Although broken, fairly robust fibular tubercle is recognized on the anterior surface of the bone, giving the proximal portion of the fibula a subtriangular cross-section.

THE POSTCRANIUM OF TRITYLODONTIDS: A COMPARATIVE ANALYSIS

For the comparative exercise, we followed the descriptions and illustrations previously published (mainly Young, 1947; Kühne, 1956; Fourie, 1962; Sun and Li, 1985; Maisch et al., 2004; Sues and Jenkins, 2006; Sullivan et al., 2013) regarding the anatomical traits of tritylodontids other than *Tritylodon*. Additionally, we personally analyzed a positive cast of the left natural mould of NMQR 1272, the holotype and only specimen of *Tritylodontoideus maximus*. The cast is part of the collection of the Evolutionary Studies Institute, University of the Witwatersrand, Johannesburg. Unfortunately, the cast of the right natural mould of this specimen, preserving the major part of the skeleton, was not available at the collection of the mentioned institution. We also studied several specimens of *Oligokyphus* housed in the collection of the Natural History Museum of London and the Cambridge University Museum of Zoology. Material of *Kayentatherium* (specimen MCZ8812) was studied at the Museum of Comparative Zoology, Harvard University, Massachusetts. FA also had access to postcranial material of *Bienotherium* sp. that was on loan to James Hopson at the University of Chicago. In order to ease reading, except when indispensable, we will avoid including these references and specifying the specimens analyzed throughout the comparisons that follow.

There are four described species of the Chinese genus *Bienotheroides*: *B*. *wanhsienensis* Young, 1982; *B*. *zigongensis* Sun, 1986; *B*. *ultimus* Maisch et al., 2004; and *B*. *shartegensis* Watabe et al., 2007. The identification of these taxa is based on craniodental features, whereas their postcranial anatomy is poorly understood. Sun and Li (1985) presented the most complete description of the postcranial anatomy of *Bienotheroides*, on the basis of three different specimens; however, specific identification was possible only for IVPP-V4734, the type specimen of *Bienotheroides wanhsienensis*, because the other specimens were incompletely prepared. Maisch et al. (2004) described the fragmentary postcranial skeleton of *Bienotheroides ultimus*. These authors stated that the postcranial anatomy of *Bienotheroides ultimus* was different from that of the specimens published by Sun and Li (1985). Surprisingly, in their discussion of the postcranial characteristics, Maisch et al. (2004) referred to the material described by Sun and Li (1985) as *Bienotheroides zingongensis* instead of *Bienotheroides* sp. or *B*. *wanhsienensis* as in the original publication, without providing any justification for this identification. To avoid any confusion regarding this issue, we will make explicit the specimen number when referring to the specimens described by Sun and Li (1985).

Axial skeleton

Atlas-axis complex. *Tritylodon* shares with other tritylodontids the presence of a strongly projecting dens. The degree of anterior projection of this structure is most similar to that observed in *Bienotheroides* (IVPP-V4734). In *Kayentatherium* and *Oligokyphus*, similar to the condition of the basal mammaliaform *Morganucodon* (see Jenkins and Parrington, 1976: Fig. 1f-h), the dens is more projected than in *Tritylodon* or *Bienotheroides* (IVPP-V4734).

Fusion of the atlas centrum to that of the axis is a variable feature among non-mammaliaform cynodonts (e.g., Jenkins, 1971). *Tritylodon* shares with *Bienotheroides* (IVPP-V4734), *Oligokyphus*, and *Morganucodon* (see Jenkins and Parrington, 1976: Fig. 1f-h) the fused condition of these elements, which are not fused in *Kayentatherium*.

The fused centrum of the atlas and axis is remarkably compressed dorsoventrally in *Tritylodon*. The same condition is observed in *Oligokyphus*, *Bienotheroides* (IVPP-V4734), *Kayentatherium*, and an indeterminate tritylodontid (Sues and Jenkins, 2006: fig. 5.1E), and has also been reported in *Morganucodon* as a “shape characteristic of later mammals” by Jenkins and Parrington, 1976 (see Jenkins and Parrington, 1976: fig.1f).

A keel on the ventral surface of the atlanto-axial centrum has been reported in a number of non-mammaliaform cynodonts (e.g. Kühne, 1956; Jenkins, 1971; Sun and Li, 1985; Sues and Jenkins, 2006). In *Bienotheroides* (IVPP-V7434), this keel is restricted to the axial centrum as observed in *Tritylodon* specimen BP/1/4782. On the other hand, a similar condition to that of *Tritylodon* specimen BP/1/5167 (i.e. with the ventral keel extending onto the atlantal portion of the centrum) is known in *Oligokyphus* and *Megazostrodon* (BP/1/4983). The indeterminate tritylodontid analyzed by Sues and Jenkins (2006; MCZ8839) includes an isolated atlantal centrum that bears a well defined mid-ventral keel, but it is unknown if a keel was also present on the axial body. The atlantal and axial centra of *Kayentatherium* are strongly constricted ventrally, defining an elevated central area, but do not bear a crest-like structure like that observed in other tritylodontids. Despite being partially obscured by deformation, the differences between *Tritylodon* specimens BP/1/4782 and

BP/1/5167 regarding the extent of this ventral keel on the atlanto-axial centrum represents previously unnoticed intraspecific variation in this feature.

Similar to *Tritylodon*, the presence of parapophyses in the atlanto-axial centra can be recognized in *Kayentatherium* and *Oligokyphus*, but not in *Bienotheroides* (IVPP-V7434). Parapophyses are also recognizable in *Galesaurus* (see Jenkins, 1971), but they are restricted to the atlas intercentrum.

***Post-axial cervical vertebrae*.** Similar to *Kayentatherium* and *Oligokyphus*, *Tritylodon* lacks independently ossified intercentra in the postaxial cervicals, unlike the condition observed in *Thrinaxodon* (see Jenkins, 1971). The proportions of the postaxial cervical centra of *Tritylodon* are similar to those observed in *Bienotheroides ultimus* and *Oligokyphus*, in the c3 of *Bienotheroides* (IVPP-V4734), and also in *Thrinaxodon* (see Jenkins, 1971). On the other hand, the postaxial cervical centra of *Kayentatherium* and the c4 of *Bienotheroides* (IVPP-V4734) are extremely short anteroposteriorly (approximately three times shorter than wide laterally). *Tritylodon* shares with *Bienotheroides ultimus* the presence of anteriorly and posteriorly flat (platycoelous) postaxial cervical centra, whereas the centra in this part of the column are procoelous in *Oligokyphus* and amphicoelous in *Kayentatherium*. The parapophyses on the postaxial cervical centra of *Tritylodon* are similarly placed to those of *Kayentatherium*. In these genera, the parapophyses of anterior postaxial vertebra are anteroventrally positioned and become successively more dorsal posteriorly. *Oligokyphus* differs from *Tritylodon* and *Kayentatherium* in that the parapophyses are situated slightly posterior to the anterior margin of the centrum. *Tritylodon*, *Kayentatherium*, and *Oligokyphus* lack parapophyseal facets at the posterior margins of the centra, implying that the cervical ribs did not articulate intervertebrally in these taxa. By contrast, postaxial cervical centra of *Thrinaxodon* have dorsally positioned parapophyseal facets both anteriorly and posteriorly (see Jenkins, 1971).

Unlike in *Kayentatherium*, in which all cervicals bear a ventral keel, only the anterior cervicals (c3-4) of *Tritylodon* are keeled. A mid-ventral keel is also known in *Oligokyphus*, but it is not possible to ascertain if this structure was present in all the cervical vertebrae. In *Bienotheroides ultimus*, the ventral surfaces of the cervical vertebrae are rather flat, and either lack a keel or bear only a slight one. *Tritylodon* also differs from *Kayentatherium* in that the postzygapophyses do not project so posteriorly beyond the vertebral centra in the former taxon. Additionally, the postzygapophyses of *Tritylodon* do not flare laterally, as seen in dorsal view, as much as in *Bienotheroides* (IVPP-V7906).

***Dorsal vertebrae*.** The centra of the anterior dorsal vertebrae of *Tritylodon* are slightly longer than broad, whereas those of *Oligokyphus* are broader than long and those of *Kayentatherium* are laterally compressed and long anteroposteriorly. On the other hand, more posterior dorsal centra are consistently longer anteroposteriorly than broad laterally in *Tritylodon*, *Kayentatherium*, and *Oligokyphus*. *Bienotheroides* (IVPP-V7906) differs from *Tritylodon* in that the dorsal vertebral centra are broader than long. In *Bienotheroides ultimus*, the thoracic vertebrae are only slightly longer than broad, similar to the anterior dorsal vertebrae of *Tritylodon*. In *Kayentatherium* and *Oligokyphus*, unlike in *Tritylodon*, mid-ventral keels are present at least in the anteriormost dorsal vertebrae. *Bienotheroides ultimus* dorsal vertebrae lack mid-ventral keels, but it is not possible to be certain if the known elements include the first dorsal. Dorsal vertebrae of *Tritylodon*, *Kayentatherium*, and *Oligokyphus* share the presence of a crest connecting the transverse process with the parapophyseal facet.

The posterior-most dorsal vertebra available of *Tritylodon* (BP/1/4785g) is very similar to that what was interpreted as the dorsal vertebrae 16 of *Oligokyphus*. These elements share the presence of low neural arch, laterally and slightly anteriorly oriented transverse processes at mid-length of the vertebral centrum, postzygapophyses and neural spine posterior to the vertebral centrum, horizontal prezygapophysis, and the absence of anteriorly projecting prezygapophyseal processes. On the other hand, the centrum of *Tritylodon* BP/1/4785g is almost as long as wide whereas the width of the centrum of the 16 dorsal vertebrae of *Oligokyphus* is two-thirds of its length.

Appendicular skeleton

Scapula. Tritylodontids are characterized by an anteroposteriorly expanded scapular blade clearly different from that of other non-mammaliaform cynodonts (e.g., Jenkins, 1971). A triangular scapular blade with a remarkably long dorsal margin distinguishes *Tritylodon* and *Kayentatherium* in particular. In *Bienotheroides* (IVPP-V7905), the scapular blade is also anteroposteriorly expanded as in other tritylodontids, but the anterodorsal portion of the blade is poorly developed. As a result, the scapula of *Bienotheroides* does not appear triangular in lateral aspect, and has a convex anterior margin and a concave posterior one. The incompleteness of known scapulae of *Oligokyphus* precludes proper comparisons involving this genus.

The scapula of *Tritylodon* differs from that of *Kayentatherium* in lacking (a) a well developed postscapular fossa visible in lateral aspect, (b) a rugose muscular insertion area on the scapular spine, (c) a groove for the insertion of the *caput scapularis* of the *M. triceps brachii*, and (d) a robust plate-like acromion process with a distinct clavicular facet. *Tritylodon* is similar to *Bienotheroides* (IVPP-V7905) in that the acromion process is more slender and finger-like, and not as ventrally oriented, as in *Kayentatherium*. Similar to *Kayentatherium*, *Oligokyphus* has a ventroanteriorly oriented acromion process and a purportedly discernible area for the insertion of the *caput scapularis* of the *M. triceps brachii*. The only described scapula of *Bienotheroides ultimus* is a fragment of the glenoid region (Maisch et al., 2004) which is notably similar to that of *Tritylodon*. A close comparison between these taxa leads us to question whether the fragmentary scapula described and illustrated by Maisch et al. (2004: Fig. 3b-c) as a left element could be instead a right one. The scapula of *Bienotheroides* (IVPP-V7905; see Sun and Li, 1985: Fig. 6a) has a relatively larger infraspinous fossa than that of *Tritylodon*. Although a supraspinous fossa is present in some specimens of *Bienotheroides* (IVPP-V7905), this feature is not visible in lateral aspect as in *Tritylodon* and *Kayentatherium*. Additionally, in *Bienotheroides* (IVPP-V7905) the dorsoposterior corner of the scapular blade is more posteriorly projected than in *Tritylodon*. In *Kayentatherium*, a much better developed posterior projection of the dorsoposterior corner of the scapular blade is present.

***Coracoid*.** The coracoid of *Tritylodon* and *Kayentatherium* is about half as long as the scapula and also more slender, although the coracoid is stouter in *Tritylodon* than in *Kayentatherium*. According to the reconstruction by Sun and Li (1985: Fig. 8), the coracoid in *Bienotheroides* (IVPP-V7905 and IVPP-V7906) had similar proportions to that of *Tritylodon*. The glenoid facet of the coracoid is dorsally oriented in *Tritylodon*, whereas in *Kayentatherium* the facet faces mainly posterolaterally with a minor dorsal component. In *Tritylodon*, the posterior portion of the coracoid, corresponding to the tuberosity for the origin of the triceps, is rectangular in lateral view and somewhat robust. In *Kayentatherium*, by contrast, the coracoid tapers to an acuminate posterior end.

***Procoracoid*.** The procoracoid of *Tritylodon* is very similar to that of *Kayentatherium* in general shape, relative size, and the position of the procoracoid foramen. Comparisons with the scapula, coracoid, and procoracoid of *Oligokyphus* are not presented here due to uncertainties concerning the reconstruction provided by Kühne (1956).

***Humerus*.** The humerus of *Tritylodon* is more slender than those of *Bienotherium*, *Bienotheroides ultimus*, and *Kayentatherium*, and more robust than that of *Oligokyphus*. Measuring from the distal inflexion of the deltopectoral crest to the proximal rim of the entepicondylar foramen, the humeral diaphysis of *Tritylodon* is about as long as those of

Cynognathus and *Thrinaxodon* but short when compared to those of other tritylodontids such as *Bienotherium*, *Bienotheroides ultimus*, *Kayentatherium,* and *Oligokyphus* (Tab. 6). The proximal and distal expansions of the humerus in *Tritylodon* are most closely comparable in size to those in *Cynognathus* and *Thrinaxodon* (Tab. 6). In relative terms, the width between the greater and lesser tuberosities in *Tritylodon* is greater than the equivalent measurement in *Oligokyphus* but smaller than the equivalent measurement in *Bienotherium*, *Bienotheroides ultimus* and *Kayentatherium* (Tab. 6). The width across the epicondyles in available *Tritylodon* specimens is similar to that measured in *Bienotheroides ultimus*, *Kayentatherium*, and *Oligokyphus*, but smaller than that of *Bienotherium* (Tab. 6). The robust lesser tuberosity region (proximomedial portion of the humerus) of *Tritylodon* is comparable to that of *Bienotherium* and *Bienotheroides ultimus*. On the other hand, this area is less well developed in *Kayentatherium* and *Oligokyphus*. In *Kayentatherium* and *Tritylodontoideus*, the deltopectoral crest is better developed than in the remaining tritylodontids, including *Tritylodon*. The entepicondyle of *Tritylodon* is narrower proximodistally than that of *Bienotherium* and *Kayentatherium*, similar to that of *Bienotheroides ultimus* and *Oligokyphus*. Unlike in *Tritylodon*, *Bienotherium*, *Bienotheroides* (IVPP-V7906), and *Bienotheroides ultimus*, the capitulum appears relatively well developed in *Kayentatherium* and *Oligokyphus* in dorsal view.

Ulna. The lateral surface of the olecranon of *Tritylodon* has a convex anterior margin in contrast to the straight anterior margin observed in *Bienotheroides ultimus, Kayentatherium,* and *Oligokyphus* . The morphology of the olecranon process in *Bienotheroides* (IVPP-V7905) is straight to slightly concave as shown in the published figure (Sun and Li, 1985: Fig. 10). In *Tritylodon*, the facet for the ulnar condyle of the humerus is almost perfectly aligned with the long axis of the bone, whereas in *Kayentatherium* and *Oligokyphus* the long axis of the facet is diagonally oriented in anterior view. Additionally, the facet for the radial condyle of the humerus and the radial notch both face mainly anteriorly in *Kayentatherium* and *Oligokyphus*, unlike in *Tritylodon*. Compared to *Tritylodon* and other trtylodontodids, the olecranon of *Tritylodontoideus* is much higher.

Radius. *Tritylodon* differs from *Kayentatherium* and *Oligokyphus* in having a less well developed facet for the ulna on the medial aspect of the radius. In *Tritylodon* the bicipital tuberosity is more distally placed than in *Kayentatherium*. Unlike in *Kayentatherium*, there is no evident radial fossa in *Tritylodon* and *Oligokyphus*.

Ischium. The ischial buttress and the supraacetabular crest are better developed in the Lufeng tritylodontid (CXPM-C2019 2A235) than in *Tritylodon*. The neck of the ischium appears less constricted in *Tritylodon* than in *Oligokyphus*, *Tritylodontoideus*, and CXPM-C2019 2A235, although *Bienotheroides ultimus* resembles *Tritylodon* in this respect. *Tritylodon* shares with CXPM-C2019 2A235 the absence of a groove on the dorsal surface of the neck, differing from other tritylodontids. *Tritylodon*, *Bienotheroides ultimus*, and CXPM-C2019 2A235 differ from *Dinnebitodon* (see Sues and Jenkins, 2006: Fig. 5.16d) and *Oligokyphus* in that the dorsal margin of the ischium appears less concave in medial/lateral view in the former group of taxa. On the other hand, *Tritylodontoideus* is unique among tritylodontids in that the dorsal margin of the ischium appears dorsally convex in medial aspect. In *Tritylodon* and *Bienotheroides ultimus*, the ischial tuberosity is less dorsally prominent than in *Oligokyphus* and CXPM-C2019 2A235. In *Tritylodontoideus*, the ischial tuberosity is even less dorsally prominent than in *Tritylodon* or *Bienotheroides ultimus*. The ischial plate of *Tritylodon* is broader anteroposteriorly than those of *Oligokyphus*, *Tritylodontoideus*, and CXPM-C2019 2A235. We interpret the obturator foramen in *Tritylodon* as relatively small and oval, being longer anteroposteriorly than dorsoventrally. By contrast, the obturator foramen is large and almost circular in *Oligokyphus*, and dorsoventrally elongated in *Tritylodontoideus* and CXPM-C2019 2A235. Although incomplete, the obturator foramen of *Dinnebitodon* was interpreted as being large (Sues and Jenkins, 2006), thus differing from the condition inferred for *Tritylodon*. The ischium CXPM-C2019 2A235 shows a unique dorsal shelf (Sullivan et al., 2013: Fig. 3n–o) never reported previously for any cynodont, including mammals. We believe that this structure is possibly a consequence of taphonomic deformation.

Femur. The proximal portion of the femur of *Tritylodon* is very similar to that of *Kayentatherium* as illustrated by Sues and Jenkins (2006: Fig. 5.17), but the proximal end is more lateromedially expanded relative to the diaphysis in *Tritylodon*. A fossa for the adductor musculature like that described by Jenkins (1971) is not present in any described tritylodontid. The notches between the trochanters and the femoral head are similarly shaped in *Tritylodon* and *Kayentatherium*. In *Oligokyphus*, these notches are narrower. In *Bienotheroides* (IVPP-V7906), the notch between the head and the greater trochanter is less deep, and the one separating the head from the lesser trochanter is broader, than in *Tritylodon*. The greater and lesser trochanters are similarly oriented in *Tritylodon*, *Kayentatherium*, and *Oligokyphus*. In the Lufeng tritylodontid (CXPM-C2019 2A235), the greater trochanter is more proximally, and the lesser trochanter more medially directed. In *Bienotherium*, the greater trochanter points somewhat proximolaterally and the lesser trochanter is medially oriented. In *Bienotheroides* (IVPP-V7906), the greater trochanter is similar in orientation to that of *Tritylodon* but the lesser trochanter is slightly medially directed. The distal portion of the femur of *Tritylodon*, *Bienotherium*, *Kayentatherium*, *Oligokyphus*, and the Lufeng tritylodontid flares more laterally than medially, but it is almost symmetrical in ventral/dorsal aspect in *Bienotheroides* (IVPP-V7906). The proximal width to total femoral length ratio for the femur is similar among most tritylodontids (*Bienotherium*, 37%; *Bienotheroides* IVPP-V7906, 36%; *Kayentatherium*, 38%; and *Oligokyphus*, 37.7%), although in the Lufeng tritylodontid the proximal width of the femur is only 30.5% of the total length of the bone. Compared to the proximal end, the distal end of the femur is less expanded in proportion to femoral length in some tritylodontids (*Bienotherium*, 31.7%; *Bienotheroides* IVPP-V7906, 31.6%; and *Oligokyphus*, 27%), whereas the proximal and distal portions of the femur are almost equally expanded in *Kayentatherium* (37%) and the Lufeng tritylodontid (31%).

Tibia. As preserved, the tibia of *Tritylodon* is most similar to those of *Bienotherium* and *Bienotheroides ultimus*. These taxa differ from *Kayentatherium* and *Oligokyphus* in lacking a well developed cnemial crest, and in that the proximal portion of the tibia is less posteriorly prominent.

Outside of Africa: the purported* Tritylodon *remains from Argentina

Bonaparte (1971) succinctly described a few postcranial elements of a non-mammaliaform cynodont from the Los Colorados Formation (Norian, La Rioja Province, Argentina), which he assigned to the Tritylodontidae and tentatively to the genus *Tritylodon*. If Bonaparte's (1971) identification is correct, these remains would represent the oldest record of tritylodontids, extending the stratigraphic range of the clade into the Norian, as well as the only documentation of *Tritylodon* outside of Africa and of any tritylodontid in South America.

According to Bonaparte (1971), part of the specimen was lost during the excavation process and only the proximal portion of a femur and a tibia, the distal portion of a humerus and a fibula, and two articulated dorsal vertebrae were recovered (Figs. 12.1–6, 13). Two additional articulated vertebrae (Fig. 12.7–10), not mentioned by Bonaparte (1971), are also thought to be part of this specimen as they correspond in size and preservation to the other bones and are kept in the same box. As noted by Bonaparte (1971), the tibia and fibula are notably larger than the humerus and femur. Proportions between the femur, humerus, and vertebrae of PVL3849 are similar to those observed in specimens of *Tritylodon*, suggesting that these elements are part of the same individual to the exclusion of the tibia and fibula, which would represent a second individual under the same collection number (PVL3849).

Bonaparte (1971) described two articulated vertebrae that he interpreted as dorsals (Fig. 12.1–6). Among the African specimens of *Tritylodon* analyzed here, these vertebrae are most comparable to BP/1/4785g, a posterior dorsal vertebra, and to the dorsal vertebra 16 of *Oligokyphus* (according to Kühne, 1956). Similar to BP/1/4785g, the vertebrae described by Bonaparte (1971) have dorsoventrally compressed vertebral bodies whose flat ventral surfaces lack mid-ventral keels (Fig. 12.1–6). Furthermore, the anterior portion of the body is more expanded laterally than the posterior one (Fig. 12.3, 6). These vertebrae also share the presence of a low neural arch with the prezygapophyseal facets situated just anterior to the bases of the transverse processes on the neural arch (Fig. 12.1–2, 4–5). On the other hand, the described vertebrae of PVL3849 differ from BP/1/4785g in that they are spool-shaped, lack parapophyses, have laterally and posteriorly oriented transverse processes (rather than slightly anteriorly oriented ones), have prezygapophyseal facets that are slightly inclined rather than horizontal, and in that the postzygapophysis and neural spine are not completely posterior to the vertebral centrum (Fig. 12.1–2, 4–5). Although somewhat similar to confirmed African specimens of *Tritylodon*, especially BP/1/4785g, the described vertebrae of PVL3849 cannot be unambiguously assigned to this taxon as no diagnostic characters have been identified in the vertebrae. In our opinion, despite Bonaparte’s (1971: 168) statement to the contrary, published vertebrae of *Bienotherium* (see Young, 1947) are not comparable to either BP/1/4785g or the described vertebrae of PVL3849.

The two articulated vertebrae included in PVL3849 but not mentioned by Bonaparte mainly comprise the centra, although the left side of the neural arch and spine is partly preserved in the more posterior vertebra (Fig. 12.7–10). On the basis of their morphology, we interpret them as dorsals, situated more anteriorly than those described by Bonaparte (1971).

The centra are anteroposteriorly long, almost twice the length of the previously described elements, and dorsoventrally low. They are not spool-shaped, although the central portion of each vertebra is somewhat laterally and ventrally constricted relative to the anterior and posterior margins. A mid-ventral keel is not present. The preserved neural spine is laterally compressed, rectangular in lateral view, inclined posteriorly at approximately 45º to the horizontal, and does not taper distally (Fig. 12.7–10). Whether rib facets are present on the vertebral bodies is not clear. These vertebrae are roughly similar to dx8 of specimen BP/1/4785 and the more posterior dorsal BP/1/4785i of *Tritylodon*. These vertebrae of PVL3849 are also similar to d11-12 of *Kayentatherium* (see Sues and Jenkins, 2006), but in the later taxon the d11–12 centra are comparatively shorter. Nevertheless, it has to be kept in mind that the lack of diagnostic characters precludes an unambiguous taxonomic assignation.

The distal portion of the left humerus of PVL3849 presents many differences from African specimens of *Tritylodon* and other tritylodontyids. Contrary to what is observed in *Tritylodon* and other tritylodontids (i.e., *Bienotherium*, *Bienotheroides* [V7906], *Bienotheroides ultimus*, *Kayentatherium*, and *Oligokyphus*), the ulnar condyle of PVL3849 is larger and more distally prominent than the capitulum (Fig. 13.1–4). Moreover, when compared to the maximum width of the distal portion of the humerus, the capitulum and ulnar condyle of PVL3849 are relatively larger than in other tritylodontids. The triangular fossa proximal to the capitulum that can be seen in ventral view in African specimens of *Tritylodon*, *Bienotherium*, *Bienotheroides* (V7906), *Bienotheroides ultimus*, *Kayentatherium*, and *Oligokyphus* is not so well developed in PVL3849 (Fig. 13.3–4). Dorsally, the capitulum, similar to *Bienotherium* and the African specimens of *Tritylodon*, is not developed in PVL3849 (Fig. 13.1–2), unlike in *Kayentatherium* and *Oligokyphus*. In *Bienotheroides ultimus* and *Bienotheroides* (V7906), a trochlear facet is present dorsally, but the capitulum and ulnar condyle are not conspicuous (see Sun and Li, 1985: Fig. 9d; Maisch et al., 2004:

Figs. 3d, 4d). In PVL3849, the ulnar condyle is relatively larger than in tritylodontids as observed dorsally. The olecranon fossa in PVL3849, similar to that in *Kayenthaterium*, is very shallow (Fig. 13.1–2), unlike in the African specimens of *Tritylodon*, *Bienotherium*, *Bienotheroides ultimus*, and *Oligokuphus*. Unlike in *Bienotherium*, *Bienotheroides* (V7906), *Kayentatherium*, *Oligokyphus*, and *Tritylodon*, the ectepicondyle in PVL3849 is poorly developed and the capitulum almost reaches the lateral margin of the ventral surface of the humerus (Fig. 13.1–4), as already noted by Bonaparte (1971). In *Bienotheroides ultimus*, the ectepicondyle is larger than in PVL3849 but, when compared to other tritylodontids, this structure is not so well developed and the capitulum is relatively laterally placed in *Bienotheroides ultimus* (see Maisch et al., 2004: Figs. 3d, 4c). In PVL3849, the entepicondylar foramen opens ventrally into a relatively narrow groove that continues to the distal margin the humerus and separates the ulnar condyle from the entepicondyle (Fig. 13.3–4). The distal portion of the humerus of PVL3849 is similar to that of the tritheledontids *Irajatherium* (Martinelli et al., 2005; Oliveira et al.; 2011) and *Pachygenelus* (Gow, 2001; LCG pers. obs.), although the distal portion of the humerus of *Irajatherium* appears more mediolaterally expanded than that of PVL3849 or *Pachygenelus*. PVL3849 shares with tritheledontids the presence of an ulnar condyle larger and more distally prominent than the capitulum, the shallow triangular fossa proximal to the capitulum in ventral aspect, the poorly developed olecranon fossa, the laterally placed capitulum, the reduced ectepicondyle, and the hook-like entepicondyle. Unlike *Irajatherium*, the capitulum is not developed dorsally in PVL3849 and *Pachygenelus* (Fig. 13.1–2; Oliveira et al.; 2011).

The left femur of PVL3849 (Fig. 13.5–8) is roughly similar to that of tritylodontids, although some differences are recognized. The tips of the greater and lesser trochanters of PVL3849 are not as separated proximodistally as in tritylodontids. The greater trochanter of PVL3849 is less robust and not so extensive proximodistally as in tritylodontids. In PVL3849, the greater trochanter is lower and points laterally as well as proximally, differing from the taller, proximally projected greater trochanter of tritylodontids. The greater trochanter in PVL3849 is separated from the femoral head by a broader and shallower notch than that observed in tritylodontids with the exception of *Bienotheroides* (V7906). The lesser trochanter of PVL3849 is more sharply pointed than in the African specimens of *Tritylodon*, *Bienotherium*, *Kayentatherium*, and the Lufeng tritylodontid (CXPM C2019 2A235), similar to *Bienotheroides* (V9706), and more rounded than in *Oligokyphus*. Unlike tritylodontids, except *Bienotheroides* (V7906) and the Lufeng form, the lesser trochanter of PVL3849 projects medially instead of proximomedially. In *Bienotherium*, the lesser trochanter projects somewhat mediodistally (see Young, 1947: fig. 20A). Similar to tritylodontids, in PVL3849 the intertrochanteric fossa is shallow, with a poorly defined distal margin (Fig. 13.5–6). On the other hand, distal to the intertrochanteric fossa, a slightly depressed central area might represent a fossa for the adductor musculature (as interpreted by Jenkins, 1971; Fig. 13.5–6), a structure that was not identified in tritylodontids. The femur of PVL3849 as well as that of tritylodontids is notably different from that of the Brazilian *Irajatherium*, the only tritheledontid taxon for which the femur has been described (Martinelli et al., 2005; Oliveira et al., 2011). Unlike PVL3849 and tritylodontids, the femur of *Irajatherium* has an almost no medially projected head, lacks a conspicuous neck, and presents a thin greater trochanter which is rounded, laterally projected, and continuous with the femoral head. The lesser trochanter of *Irajatherium* is medially oriented as in PVL3849 but, unlike the Argentinean specimen and tritylodontids, it is not separated from the femoral head by a well defined notch. Additionally, in *Irajatherium*, there is a concave area dorsally, purportedly for the attachment of the *M. pubo-ischio-femoralis internus* (Martinelli et al., 2005), that has not been identified in PVL3849 or tritylodontids.

The tibia mentioned by Bonaparte (1971) is a well preserved proximal portion of a right element (Fig. 13.9–18). Regrettably, the only tibial fragment belonging to an African specimen of *Tritylodon* (BP/1/5167) is not well preserved precluding significant morphological comparisons. Among non-mammaliaform cynodonts, the tibia of PVL3849 is most similar to those of tritylodontids, particularly *Kayentatherium*, although some differences are present. The proximal portion of the tibia of PVL3849 has a triangular outline in anterior/posterior view (Fig. 13.9–12). The proximal articular surface is broader lateromedially than anteroposteriorly, and bears two oval articular facets for the femoral condyles. These facets are concave and separated by a low broad ridge, the lateral facet being larger than the medial one (Fig. 13.17–18). A very robust tibial tuberosity, which is not present in other tritylodontids (i.e., *Oligokyphus* and *Kayentatherium*), projects anteriorly from the proximal region of the tibia (Fig. 13.9–10). A thin, low cnemial crest runs distally and medially from the tibial tuberosity to the incompletely preserved medial margin, defining a triangular fossa that faces anteromedially and could represent the origin area of the *M. tibialis anterior*, as suggested for *Kayentatherium* (Sues and Jenkins, 2006) and *Oligokyphus* (Kühne, 1956). In PVL3849 the cnemial crest is shorter than in *Kayentatherium* and *Oligokyphus*, reaching the medial margin of the bone close to the proximal surface (Fig. 13.9–10). Consequently, the fossa for the *M. tibialis anterior* is not so distally extensive as in *Kayentatherium* and *Oligokyphus*. The posterior surface of the preserved proximal region of the tibia of PVL3849 is evenly concave (Fig. 13.11–12). In *Kayentatherium*, however, the posterior surface of the tibia bears convex lateral and medial areas flanking a narrow central region.

Only the distal portion of the right fibula of PVL3849 has been recovered (Fig. 13.19–22). The shaft of the fibula is almost straight and has a triangular cross-section as described by Jenkins (1971) for *Cynognathus*/*Diademodon*. The distal portion of the fibula has a triangular outline in lateral view (Fig. 13.21–22) and expands medially as seen in anterior view (Fig. 13.19–20). A ridge is present on the anterior edge of the fibula, and ends distally in an anteriorly projecting tuberosity (Fig. 13.19–20). The anterior ridge and the medial border of the fibula flank a triangular, slightly concave region (Fig. 13.19–20). The distal portion of the fibula is laterally convex in anterior view. The medial end of the fibula projects more distally than the lateral region, as can be seen in anterior view (Fig. 13.19–20). A robust ridge is present on the lateral face of the distal portion of the bone (Fig. 13.21–22).

After this comparison of the limited remains of PVL3849 with the African species *Tritylodon longaevus* and other tritylodontids, we consider that the material from the Los Colorados Formation of Argentina should be regarded as an undetermined non-mammaliaform cynodont different from *Tritylodon longaevus* or any other tritylodontid. Comparisons with the tritheledontids *Irajatherium* and *Pachygenelus*, show that tritheledontid affinities of PVL3849 cannot be ruled out given the similarities in the anatomy of the humerus. On the other hand, the femur of PVL3849 differs greatly from that of *Irajatherium*. The only other cynodont record for the Los Colorados Formation comprises two imperfectly preserved skulls of the tritheledontid *Chaliminia musteloides* (see Bonaparte, 1980; Martinelli and Rougier, 2007; Arcucci et al., 2004). PVL3849 is a much larger individual than those represented by the known specimens of *Chaliminia*, and is probably not conspecific with them. The available evidence points to the presence of a still unrecognized taxon from the Los Colorados Formation.

DISCUSSION

The monophyly of tritylodontids is universally accepted (Liu and Olsen, 2010) whereas the issue of whether they are cynognathians or probainognathians has been debated (see Sues and Jenkins, 2006; Liu and Olsen, 2010). Several skeletal characteristics seen in tritylodontids have been suggested to link them to basal mammaliaforms (Kemp, 1982, 1983, 1988), whereas other authors have regarded tritylodontids as nested among cynognathians and considered the features shared with mammaliaforms to be convergent in nature (Sues, 1985; Sues and Jenkins, 2006). Moreover, Sues and Jenkins (2006) stated that some of the mammaliaform-like postcranial features recognized in tritylodontids should be regarded as independently evolved apomorphies of this group. These suggestions are supported by the phylogenetic study of Hopson and Kitching (2001), but not by that of Rowe (1988) or by the more comprehensive study of Liu and Olsen (2010). It is important to bear in mind that the postcranial skeleton of non-mammaliaform cynodonts has only been represented by a relatively small number of characters in phylogenetic studies (e.g., Rowe, 1988; Hopson and Kitching, 2001; Liu and Olsen, 2010), and that the postcranial anatomy of many non-mammaliaform cynodonts is unknown or has only been sparsely documented. Resolving these issues is beyond the scope of the present contribution.

Our survey of the postcranial anatomy of all known tritylodontids shows that several features distinguish them from most other non-mammaliaform cynodonts. The scapular blade of tritylodontids is distinctive in being anteroposteriorly broad with a triangular to near-triangular outline. The presence of postscapular and supraspinous fossae is also characteristic of the scapula of tritylodontids, although these structures have been documented in less developed form in some specimens of basal cynodonts (*Cynognathus* and *Diademodon*) and purportedly in *Probainognathus*. The procoracoid of tritylodontids is notably reduced anteroposteriorly in comparison to those of other non-mammaliaform cynodonts (e.g., Jenkins, 1971). Among non-mammaliaform cynodonts, an ossified sternum is known only in tritylodontids, as other taxa presumably had cartilaginous sterna (e.g., Jenkins, 1971). With regard to the pelvic girdle, the ilium of tritylodontids is unique in lacking a posterior lamina, and in that the anterior lamina is a low rod bearing a ridge that divides this region of the bone into dorsal and ventral portions. The ulna in tritylodontids has a well-developed olecranon process which defines a fully semicircular trochlear notch (also present in *Brasilitherium*, Bonaparte et al., 2005: Fig. 6). The femur of tritylodontids has a well-defined head and relatively proximally positioned greater and lesser trochanters, with a notch separating the head from the greater trochanter. This morphology clearly differs from that seen in other non-mammaliaform cynodonts (e.g., Jenkins, 1971; Martinelli et al., 2005).

A relatively large range of size variation is represented in tritylodontids (Tabs. 1, 3). *Kayentatherium* and *Tritylodontoideus* are the largest forms whereas *Oligokyphus* is relatively small, its skull length being only ~35% of that of *Kayentatherium* and *Tritylodontoideus*. The 3.4 kg estimated body mass of *Oligokyphus* is similar to that of the indeterminate tritylodontid from the Lufeng Formation (CXPM C2019 2A235), representing approximately 3.5% of the weight of the largest form, *Kayentatherium*. *Bienotheroides ultimus* is even smaller, with an estimated mass of 1.5 kg (Tab. 3). *Tritylodon* and the other tritylodontids with known postcranial remains represent intermediate-sized forms (Tab. 3). Given the size range recognized among tritylodontid species, it might be expected that at least some of the anatomical differences between them would be correlated with variation in body size. However, our comparative review shows that this might not be the case. Most surprisingly, large and small tritylodontid taxa (*Kayentatherium* and *Oligokyphus*, respectively) share several features of the postcranial skeleton not seen in other tritylodontids, particularly in the known limb elements. According to our study, many postcranial variations are clearly unrelated to body size whereas only a few traits of the shoulder girdle and humerus presently appear to correlate with body size (i.e., the relatively well developed deltopectoral crest observed in the humerus of *Kayentatherium* and *Tritylodontoideus*, and the well developed postscapular fossa visible in lateral aspect, the rugose muscular insertion area on the scapular spine, and the robust plate-like acromion process with a distinct clavicular facet in the scapula of *Kayentatherium*). These features seem to be related to increased muscle attachment area and separation between different muscle masses. It is worth mentioning that the finding of new and better preserved tritylodontid specimens might result in the discovery of more correspondences between size and anatomy in the future.

CONCLUSION

Tritylodon longaevus is a medium-sized tritylodontid, known from several specimens, which shares with other tritylodontids many postcranial features in addition to unique cranio-dental characteristics. A relatively large size range has been recorded among tritylodontids, but we found body size to be uncorrelated with variations in postcranial anatomy, as the smallest and largest tritylodontids have some distinctive traits in common. The sole exception was that certain features of the humerus of *Kayentatherium* and *Tritylodontoideus* and in the scapula of *Kayentatherium*, probably related to increased muscle insertion area and greater separation among muscle masses, could be linked to large body size.

Despite some differences, the postcranial anatomy of tritylodontids is noticeably different from that of other non-mammaliaform cynodonts. Comparisons of the anatomy of the femur and the distal portion of the humerus of tritylodontids and triheledontids highlight several differences between them.

A few remains from the Late Triassic (Norian) of South America (Bonaparte, 1971) have been tentatively assigned to *Tritylodon*, and would represent the oldest tritylodontid known to date if its identification is correct. This specimen would be the only record of *Tritylodon* outside of Africa, and the only one of a tritylodontid from South America. The re-description and comparative analysis of Bonaparte's (1971) specimen performed here suggest that it belongs to a taxon different from *Tritylodon longaevus* as well as other tritylodontids, and should be regarded as an undetermined non-mammaliaform cynodont until more complete remains are found. Additionally, our analysis shows that tritheledont affinities cannot be ruled out for this specimen. In any scenario, the South American specimen represents the record of a still-unknown non-mammaliaform cynodont in the Los Colorados Formation. The unknown cynodont must be larger than the tritheledontid *Chaliminia musteloides*, the only currently recognized cynodont taxon from this unit (Arcucci et al., 2004).

ACKNOWLEDGEMENTS

We thank M. Raath and B. Zipfel (Evolutionary Studies Institute, University of the Witwatersrand), J. Powell (Instituto Miguel Lillo), and J. Cundiff (Museum of Comparative Zoology, Harvard University) for granting access to the collections under their care. Dr. I. Corfe is thanked for his aid regarding the tritylodonts from Japan and Russia. The valuable comments and suggestions of the reviewers, Dr. C. Sullivan and Dr. M. Soares, and the artwork editor, Dr. A. Otero, greatly improved the quality of this paper. We also thank Dr. D. Pol and Dr. G. Rougier for their help during the editorial process. This research article was possible thanks to funding provided by the National Research Foundation of South Africa and the National Research Foundation Research Incentive to FA, PICT 2013-2701 and PIP 11220150100760CO to LCG, PICT 2014-1921 to V. Krapovicas, and the Bi-National Cooperation Project between South Africa (Department of Science and Technology to B. Rubidge) and Argentina (Ministerio de Ciencia, Técnica e Innovación Productiva to C. Marsicano). This is L.C.G.'s R-188 contribution to the IDEAN.

REFERENCES

Abdala, F. 1999. Elementos postcraneanos de *Cynognathus* (Synapsida-Cynodontia) del Triásico Inferior de la Provincia de Mendoza, Argentina. Consideraciones sobre la morfología del húmero en cinodontes. *Revista Española de Paleontología* 14: 13–24.

Angielczyk, K.D. 2004. Phylogenetic evidence for and implications of a dual origin of propaliny in anomodont therapsids (Synapsida). *Paleobiology* 30: 268–296.

Arcucci, A.B., Marsicano, C.A. and Caselli, A.T. 2004. Tetrapod association and palaeoenviroment of the Los Colorados Formation (Argentina): a significant sample from Western Gondwana at the end of the Triassic. *Geobios* 37: 557–568.

Anyonge, W. 1993. Body mass in large extant and extinct carnivores. *Journal of Zoology (London)* 231: 339–350.

Bonaparte, J.F. 1971. Los tetrápodos del sector superior de la Formación Los Colorados, La Rioja, Argentina (Triásico Superior). *Opera Lilloana* 22: 87–102.

Bonaparte, J.F. 1980. El primer ictidosaurio (Reptilia, Therapsida) de América del Sur, *Chaliminia musteloides*, del Triásico Superior de La Rioja. *2º Congreso Argentino de Paleontología y Bioestratigrafía y 1er Congreso Latinoamericano de Paleontología* (Buenos Aires), *Actas* 1: 123–133.

Bonaparte, J.F., Martinelli, A.G. and Schultz, C.L. 2005. New information on *Brasilodon* and *Brasilitherium* (Cynodontia, Probainognathia) from the Late Triassic of Southern Brazil. *Revista Brasileira de Paleontologia* 8: 25–46.

Botha, J. 2002. *The palaeobiology of the non-mammalian cynodonts deduced from bone microstructure and stable isotopes*. Ph.D. dissertation, University of Cape Town, Cape Town, 218 p. Unpublished.

Botha-Brink, J., Abdala, F. and Chinsamy-Turan A. 2012. The radiation and osteohistology of nonmammaliaform cynodonts. In: A. Chinsamy-Turan (Ed.), *Forerunners of Mammals: Radiation, Histology, Biology*, Indiana University Press, Bloomington, p. 223–246.

Broili, F. and Schröder, J. 1936. Beobachtungen an Wirbeltieren der Karrooformation. XIX. Ein neuer Fund von *Tritylodon* Owen. *Sitzungsberichte der Bayerischen Akademie der Wissenchaften, Mathematisch-naturwissenschaftliche* Abteilung 1936, p 187-256.

Broom, R. 1910. On *Tritylodon* and its relationships with the Multituberculata. *Proceedings of the Zoological Society of London* 80: 760–769.

Chinsamy, A. and Hurum, J. H. 2006. Bone microstructure and growth patterns of early mammals. *Acta Palaeontologica Polonica* 51: 325–338.

Clark, J.M. and Hopson, J.A. 1985. Distinctive mammal−like reptile from Mexico and its bearing on the phylogeny of the Tritylodontidae. *Nature* 315: 398–400.

Crompton, A.W. and Hotton, N.1967. Functional morphology of the masticatory apparatus of two dicynodonts (Reptilia, Therapsida). *Postilla* 109:1–51.

Fariña, R.A., Vizcaino, S.F. and Bargo, M.S. 1998. Body mass estimations in Lujanian (Late Pleistocene-Early Holocene of South America) mammal megafauna. *Mastozoología Neotropical* 5: 87–108.

Fourie, S. 1962. Further notes on a new tritylodontid from the Cave Sand-stone of South Africa. *Navorsinge nasionale Museum Bloemfontein* 2: 7–19.

Fourie, S. 1963. A new tritylodontid from the Cave Sandstone of South Africa. *Nature* 198: 201.

Hammer, W.R. and Smith, N.D. 2008. A tritylodont postcanine from the Hanson Formation of Antarctica. *Journal of Vertebrate Paleontology* 28: 269–273.

Ginsburg, L. 1962. *Likhoelia ellenbergeri*, tritylodonte du Trias supérieur du Basutoland (Afrique du Sud). *Annales de Paléontologie* 48: 177–194.

Gow, C.E. 1986. The side wall of the braincase in cynodont therapsids, and a note on the homology of the mammalian promontorium. *South African Journal of Zoology* 21:136–148.

Gow, C.E. 1991. Vascular system associated with the sidewall of the braincase and the prootic canals of cynodonts, including mammals. *South African Journal of Zoology* 26:140–144.

Gow, C.E. 2001. A partial skeleton of the tritheledontid *Pachygenelus* (Therapsida: Cynodontia). *Palaeontologia Africana* 37: 93–97.

Gregory, W.K. and Camp, C.L. 1918. Studies in comparative myology and osteology. No. III. *Bulletin of the American Museum of Natural History* 38: 447–563.

Hopson, J.A. and Kitching, J.W. 2001. A probainognathian cynodont from South Africa and the phylogeny of non-mammalian cynodonts. *Bulletin of the Museum of Comparative Zoology* 156:5–35.

Jasinoski, S.C. and Chinsamy, A. 2012. Mandibular histology and growth of the nonmammaliaform cynodont *Tritylodon*. *Journal of Anatomy* 220: 564–579.

Jenkins, F.A., Jr. 1971. The postcranial skeleton of African cynodonts. *Peabody Museum of Natural History Bulletin* 36: 1–216.

Jenkins, F.A., Jr. and Parrington, F.R. 1976. The postcranial skeletons of the Triassic mammals *Eozostrodon*, *Megazostrodon* and *Erythrotherium*. *Philosophical Transactions of the Royal Society of London* 273: 387–431.

Kemp, T.S. 1982. Mammal-like reptiles and the origin of mammals. Academic Press: London.

Kemp, T.S. 1983. The relationships of mammals. *Zoological Journal of the Linnean Society* 77: 353–384.

Kemp, T.S. 1988. Interrelationships of the Synapsida. In: M.J. Benton (Ed.), *The phylogeny and classification of the tetrapods, Vol.2: Mammals*, Oxford University Press, Oxford, p. 23–29.

Kemp, T.S. 2005. *The origin and evolution of mammals*. Oxford University Press, Oxford, 344 p.

Kermack, D.M. 1982. A new tritylodontid from the Kayenta Formation of Arizona. *Zoological Journal of the Linnean Society* 76: 1–17.

Kitching, J.W. and Raath, M.A. 1984. Fossils from the Elliot and Clarens formations (Karoo Sequence) of the north eastern Cape, Orange Free State and Lesotho, and a suggested biozonation based on tetrapods. *Palaeontologia africana* 25, 111–125.

Kühne, W.G. 1956. The Liassic therapsid *Oligokyphus*. British Museum of Natural History, 149 pp.

Lewis, G.E. 1986. *Nearctylodon broomi*, the first Nearctic tritylodont. In: N. Hotton III, P.D. MacLean, J.J. Roth and E.C. Roth (Eds.), *The Ecology and Biology of Mammal−like Reptiles*, Smithsonian Institution Press, Washington, p. 295–303.

Liu, J. and Olsen, P. 2010. The phylogenetic relationships of Eucynodontia (Amniota: Synapsida). *Journal of Mammalian Evolution* 17: 151–176.

Lopatin, A.V. and Agadjanian, A.K. 2008. A tritylodont (Tritylodontidae, Synapsida) from the Mesozoic of Yakutia. *Doklady Biological Sciences* 419: 279–282.

Luo, Z. and Wu, X.−C. 1994. The small tetrapods of the Lower Lufeng Formation, Yunnan, China. In: N.C. Fraser and H.−D. Sues (Eds.), *In the Shadow of the Dinosaurs—Early Mesozoic Tetrapods*, Cambridge University Press, Cambridge, p. 251–270.

Maisch, M.W., Matzke, A.T. and Sun, G. 2004. A new tritylodontid from the Upper Jurassic Shishugou Formation of the Junggar Basin (Xinjiang, NW China). *Journal of Vertebrate Paleontology* 24: 649–656.

Martinelli, A.G. and Rougier, G.W. 2007. On *Chaliminia musteloides* (Eucynodontia: Tritheledontidae) from the Late Triassic of Argentina, and a phylogeny of Ictidosauria. *Journal of Vertebrate Paleontology* 27: 442–460.

Martinelli, A.G., Bonaparte, J.F., Schultz, C.L. and Rubert, R. 2005. A new tritheledontid (Therapsida, Eucynodontia) from the Late Triassic of Rio Grande do Sul (Brazil) and its phylogenetic relationships among carnivorous non-mammalian eucynodonts. *Ameghiniana* 42: 191–208.

Matsuoka, H. and Setoguchi, T. 2000. Significance of Chinese tritylodonts (Synapsida, Cynodontia) for the systematic study of Japanese materials from the Lower Cretaceous Kuwajima Formation, Tetori Group of Shiramine, Ishikawa, Japan. *Asian Paleoprimatology* 1: 161–176.

Matsuoka, H., Kusuhashi, N. and Corfe, I.J. 2016. A new Early Cretaceous tritylodontid (Synapsida, Cynodontia, Mammaliamorpha) from the Kuwajima Formation (Tetori Group) of central Japan. *Journal of Vertebrate Paleontology*. DOI: 10.1080/02724634.2016.1112289.

Oliveira, T., Martinelli, A.G. and Soares, M. 2011. New information about *Irajatherium hernandezi* Martinelli, Bonaparte, Schultz & Rubert 2005 (Eucynodontia, Tritheledontidae) from the upper triassic (Caturrita Formation, Parana´ Basin) of Brazil. *Paläontologische Zeitschrift* 85: 67–82.

Owen, R. 1884. On the skull and dentition of a Triassic mammal (*Tritylodon longaevus*) from South Africa. *Quarterly Journal of the Geological Society of London* 40: 146–152.

Parrington, F.R. 1981. The Tritylodontoidea. *Journal of Natural History* 15: 155–159.

Ray, S., Botha, J. and Chinsamy, A. 2004. Bone histology and growth pattern of some nonmammalian therapsids. *Journal of Vertebrate Paleontology* 24: 634–648.

Ricqlès, A. De. 1969. Recherches paléohistologiques sur les os longs des Tétrapodes II, Quelques observations sur la structure des longs des Thériodontes. *Annales de Paléontologie (Vertébrés)* 55: 1–52.

Rowe, T. 1988. Definition, diagnosis and origin of Mammalia. *Journal of Vertebrate Paleontology* 8: 241–264.

Smith, R.M.H. and Kitching, J.W. 1997. Sedimentology and vertebrate taphonomy of the *Tritylodon* Acme Zone: a reworked paleosol in the Early Jurassic Elliot Formation, Karoo Supergroup, South Africa. *Palaeogeography, Palaeoclimatology*. *Palaeoecology* 131: 29–50.

Sues, H.−D. 1985. The relationships of the Tritylodontidae (Synapsida). *Zooogical Journal of the Linnean Society* 85: 205–217.

Sues, H.−D. 1986. The skull and dentition of two tritylodontid synapsids from the Lower Jurassic of western North America. *Bulletin of the Museum of Comparative Zoology* 151: 217–268.

Sues, H.-D. and Jenkins, F.A. Jr. 2006. The postcranial skeleton of *Kayentatherium wellesi* from the Lower Jurassic Kayenta Formation of Arizona and the phylogenetic significance of the postcranial features of tritylodontid cynodonts. In: M.T. Carrano, T.J. Gaudin, R.W. Blob and J.R. Wible (Eds.), *Amniote Paleobiology*. *Perspectives on the evolution of mammals, birds and reptiles*. Chicago University Press, Chicago, p. 114–152.

Sun, A.L. 1984. Skull morphology of the tritylodont genus *Bienotheroides* of Sichuan. *Scientita Sinica (Ser. B)* 27: 970–984.

Sullivan, C.; Liu, J., Roberts, E.M., Huang, T.D., Yang, C. and Zhonge, S. 2013. Pelvic morphology of a tritylodontid (Synapsida: Eucynodontia) from the Lower Jurassic of China, and some functional and phylogenetic implications. *Compte Rendus Palevol* 12: 505–518.

Sun, A.L. 1984. Askull of *Bienotheroides* of theTritylodontidae, Therapsida, Reptilia, from Sichuan Province. *Scientita Sinica (Series B)*1984: 257–268. [In Chinese].

Sun, A. and Li, Y. 1985. The postcranial skeleton of the late tritylodont *Bienotheroides*. *Vertebrata PalAsiatica* 23: 133–151. [In Chinese with English summary].

Tatarinov, L.P. and Matchenko, E.N. 1999. A find of an aberrant tritylodont (Reptilia, Cynodontia) in the Lower Cretaceous of the Kemerovo Region. *Paleontological Journal* 33: 422–428.

van Valkenburgh, B. 1990. Skeletal and dental predictors of body mass in carnivores. In: J. Damuth and B.J. MacFadden (Eds.), *Body size in mammalian paleobiology: estimation and biological implications*, Cambridge University Press, Cambridge, p. 181–205.

Watabe, M., Tsubamoto, T. and Tsogtbaatar, K. 2007. A new tritylodontid synapsi from Mongolia. *Acta Palaeontologica Polonica* 52: 263–274.

Young, C.C. 1940. Preliminary notes on the Mesozoic mammals of Lufeng, Yunnan, China. *Bulletin of the Geological Society of China* 20: 93–111.

Young, C.C. 1947. Mammal−like reptiles from Lufeng, Yunnan, China. *Proceedings of the Zoological Society of London* 117: 537–597.

Young, C.C. 1982. On a *Bienotherium*−like tritylodont from Szechuan, China. In: *Selected works of Yang Zhongjian*, Science Press, Beijing, p. 10–13. [In Chinese].

Figure captions

Figure 1. Atlas-axis complex of *Tritylodon*. **1–2, 5–6, 9–10,** BP/1/5167; **1–2,** dorsal view; **5–6,** left lateral view; **9–10,** ventral view. **3–4, 7–8, 11–12,** BP/1/4782; **3–4,** dorsal view; **7–8,** left lateral view; **11-12,** ventral view. Abbreviations: **af,** atlas arch facet; **cr,** crest representing the suture between the atlas and axis centra; **fai,** facet for atlas intercentrum; **mvk,** mid-ventral keel; **nc,** neural canal; **ns,** neural spine; **nsb,** neural spine base; **op,** odontoid process/dens; **pap,** parapophyses; **poz,** postzygapophyses; **tr,** transverse process. Scale bar = 10 mm.

Figure 2. First six cervical vertebrae of *Tritylodon* specimen BP/1/4965 in ventral view. Abbreviations: **aac,** atlas-axis centrum; **af,** atlas arch facet; **c3–6,** vertebral centrum; **cr,** crest representing the suture between the atlas and axis centra; **fai,** facet for atlas intercentrum; **mvk,** mid-ventral keel; **op,** odontoid process/dens; **pap,** parapophyses; **r,** rib fragment. Scale bar = 10 mm.

Figure 3. Cervical vertebrae of *Tritylodon*. **1–4,** BP/1/4785a; **1–2**, right lateral view of cervical vertebrae 3 and 4; **3–4,** ventral view of cervical vertebrae 3 and 4. **5–6, 9–10, 13–18,** BP/1/4785b; **5–6,** anterior view of cervical vertebra 5; **9–10,** ventral view of cervical vertebrae 5 to 7; **13–14,** dorsal view of cervical vertebrae 5 to 7; **15–16,** left lateral view of cervical vertebrae 5 to 7; **17–18,** right lateral view of cervical vertebrae 5 to 7. **7–8, 11–12,** BP/1/5167x, general views of a block with cervical vertebra 4 and a dorsal vertebra. Abbreviations: **c3–7,** vertebral centrum; **c,** centrum; **cr,** crest connecting the parapophysis with the transverse processes; **mvk,** mid-ventral keel; **nc,** neural canal; **ns,** neural spine; **pap,** parapophyses; **poz,** postzygapophyses; **pozb,** base of the postzygapophyses; **prz,** prezygapophyses; **przb,** base of the prezygapophyses; **r,** rib fragment; **tr,** transverse process. Scale bar = 10 mm.

Figure 4. Dorsal vertebrae of *Tritylodon*. **1–4,** BP/1/4785c; **1–2,** anterior view of dorsal vertebra dx1; **3–4,** posterior view of dorsal vertebra dx1. **5–8,** BP/1/4785d; **5–6,** anterior view of dorsal vertebra dx2; **7–8,** posterior view of dorsal vertebra dx2. **9–12,** BP/1/4785e; **9–10,** right lateral view of dorsal vertebrae dx3 and dx4; **11–12,** left lateral view of dorsal vertebrae dx3 and dx4. **13–16,** BP/1/4785f; **13–14,** left lateral view of dorsal vertebra dx5; **15–16,** right lateral view of dorsal vertebra dx5. **17–22,** BP/1/5167b; **17–18,** left lateral view of anterior dorsal vertebra; **19–20,** anterior view of anterior dorsal vertebra; **21–22,** posterior view of anterior dorsal vertebra; **23–24,** BP/1/4785j; general view of a block with dorsal vertebrae dx6 to dx8. **25–28,** BP/1/4785h; **25–26,** left lateral view of dorsal vertebra; **27–28,** right lateral view of dorsal vertebra. **29–32,** BP/1/4785i; **29–30,** left lateral view of dorsal vertebra; **31–32,** right lateral view of dorsal vertebra. **33–34,** BP/1/4785g, dorsal view of posterior dorsal vertebra. Abbreviations: **c,** centrum; **cr,** crest connecting the parapophysis with the transverse processes; **dx1–8,** vertebral centrum; **ivf,** inter-vertebral foramen; **na,** base of the neural arch; **nc,** neural canal; **ns,** neural spine; **pap,** parapophyses; **poz,** postzygapophyses; **prz,** prezygapophyses; **przb,** base of the prezygapophyses; **r,** rib fragment; **sc,** fragment of the ventral portion of the scapula; **tr,** transverse process. Scale bar = 10mm.

Figure 5. Caudal vertebrae of *Tritylodon*. **1–6,** BP/1/5089a; **1–2,** right lateral view; **3–4,** ventral view (anterior to the right); **5–6,** dorsal view (anterior to the right). **7–12,** BP/1/5089b; **7–8,** left lateral view; **9–10,** ventral view (anterior to the right); **11–12,** dorsal view (anterior to the right). Abbreviations: **na,** base of the neural arch; **nc,** neural canal. Scale bar = 10mm.

Figure 6. Pectoral girdle of *Tritylodon*. **1–4,** BP/1/5167, right scapula; **1–2,** lateral view; **3–4,** medial view. **5–10,** BP/1/5167, right procoracoid and coracoid; **5–6,** lateral view; **7–8,** medial view; **9–10,** posterior view. **11–16,** BP/1/5167, left procoracoid and coracoid; **11–12,** lateral view; **13–14,** medial view; **15–16,** posterior view. Abbreviations: **ac p,** acromion process; **c,** coracoid; **fl,** flange for muscular insertion; **gl f,** glenoid fossa; **gr,** groove; **is f,** infraspinous fossa; **sc f,** scapular facet; **s s,** scapular spine; **ss f,** supraspinous fossa; **pc,** procoracoid; **pc f,** procoracoid foramen; **ps f**, postscapular fossa; **tc**, tuberosity for the coracoid head of the triceps. Scale bars = 10mm.

Figure 7. Humerus of *Tritylodon*. **1–8,** BP/1/5671, left humerus; **1–2,** ventral view; **3–4,** dorsal view; **5–6,** lateral view; **7–8,** medial view. Abbreviations: **bi gr,** bicipital groove; **cp,** capitulum; **dp c,** deltopectoral crest; **ec,** ectepicondyle; **en,** entepicondyle; **en f,** entepicondylar foramen; **g t,** greater trochanter; **h h,** humeral head; **l t,** lesser trochanter; **o f,** olecranon fossa; **uc,** ulnar condyle. Scale bars = 10mm.

Figure 8. Ulna of *Tritylodon*. **1–6,** BP/1/4785, left ulna; **1–2,** lateral view; **3–4,** medial view; **5–6,** anterior view. Abbreviations: **f e,** extensor fossa; **f f,** flexor fossa; **f h,** facet for the ulnar condyle of the humerus; **f r,** radial facet; **i br,** insertion of *M. brachialis*; **ol p,** olecranon process; **r n,** radial notch. Scale bar = 10mm.

Figure 9. Radius of *Tritylodon*. **1–8,** BP/1/5167, left radius; **1–2,** anterior view; **3–4,** posterior view; **5–6,** medial view; **7–8,** lateral view. Abbreviations: **bi t,** bicipital tuberosity; **cr,** crest; **f u,** ulnar facet. Scale bar = 10mm.

Figure 10. Elements of the autopodium of *Tritylodon*. **1–2,** BP/1/4976, lateral centrale, metacarpal, and radiale. **3–10,** BP/1/5167, phalange; **3–4,** right lateral view; **5–6,** left lateral view; **7–8,** ventral view; **9–10,** dorsal view. Abbreviations: **c,** lateral centrale; **r,** radiale; **mc,** metacarpal; **gr,** groove; **l,** lip; **m l,** medial lip; **l n,** lateral notch. Scale bars = 10mm.

Figure 11. Femur, tibia, fibula, and ischium of *Tritylodon*. **1–8,** BP/1/5089, left femur; **1–2,** dorsal view; **3–4,** lateral view; **5–6,** ventral view; **7–8,** medial view. **9–12,** BP/1/5089, right tibia; **9–10,** lateral view; **11–12,** medial view. **13–14,** BP/1/5089, right fibula, anterior view.
15–18, BP/1/5269, right ischium; **15–16,** anterior view; **17–18,** medial view. Abbreviations: **a f,** acetabular facet; **fh,** femoral head; **f t,** fibular tubercle; **gr tr,** greater trochanter; **it f,** intertrochanteric fossa; **is n,** ischial neck; **is pl,** ischial plate; **is tu,** ischial tuberosity; **l tr,** lesser trochanter; **of m,** obturator foramen margin; **sa c,** supraacetabular crest. Scale bars = 10mm.

Figure 12. Dorsal vertebrae of the indeterminate eucynodont PVL3849. **1–6,** articulated dorsal vertebrae published by Bonaparte, 1971; **1, 4,** right lateral view; **2, 5,** left lateral view; **3, 6,** ventral view; **7–10,** articulated dorsal vertebrae previously unpublished; **7, 9,** right lateral view; **8, 10,** left lateral view. Abbreviations: **ns,** neural spine; **poz,** postzygapophyses; **przb,** base of the prezygapophyses; **tr,** transverse process. Scale bar = 10mm.

Figure 13. Humerus, femur, tibia, and fibula of the indeterminate eucynodont PVL3849. **1–4,** left humerus, **1–2,** ventral view; **3–4,** dorsal view; **5–8,** left femur; **5–6,** ventral view; **7–8,** dorsal view; **9–18,** right tibia; **9–10,** anterior view; **11–12,** posterior view; **13–14,** lateral view; **15–16,** medial view; **17–18,** proximal view; **19–22,** right fibula; **19–20,** anterior view; **21–22,** lateral view. Abbreviations: **c c**, cnemial crest; **cp,** capitulum; **ec,** ectepicondyle; **en f,** entepicondylar foramen; **en,** entepicondyle; **f mta**, facet for *M. tibialis anterior*; **f t**, fibular

tuberosity; **fh,** femoral head; **gr tr,** greater trochanter; **it f,** intertrochanteric fossa; **l tr**, lesser trochanter; **lff,** lateral facet for femoral condyle; **mff,** medial facet for femoral condyle; **o f,** olecranon fossa; **r,** ridge; **t t**, tibial tuberosity; **uc,** ulnar condyle. Scale bars = 10mm.

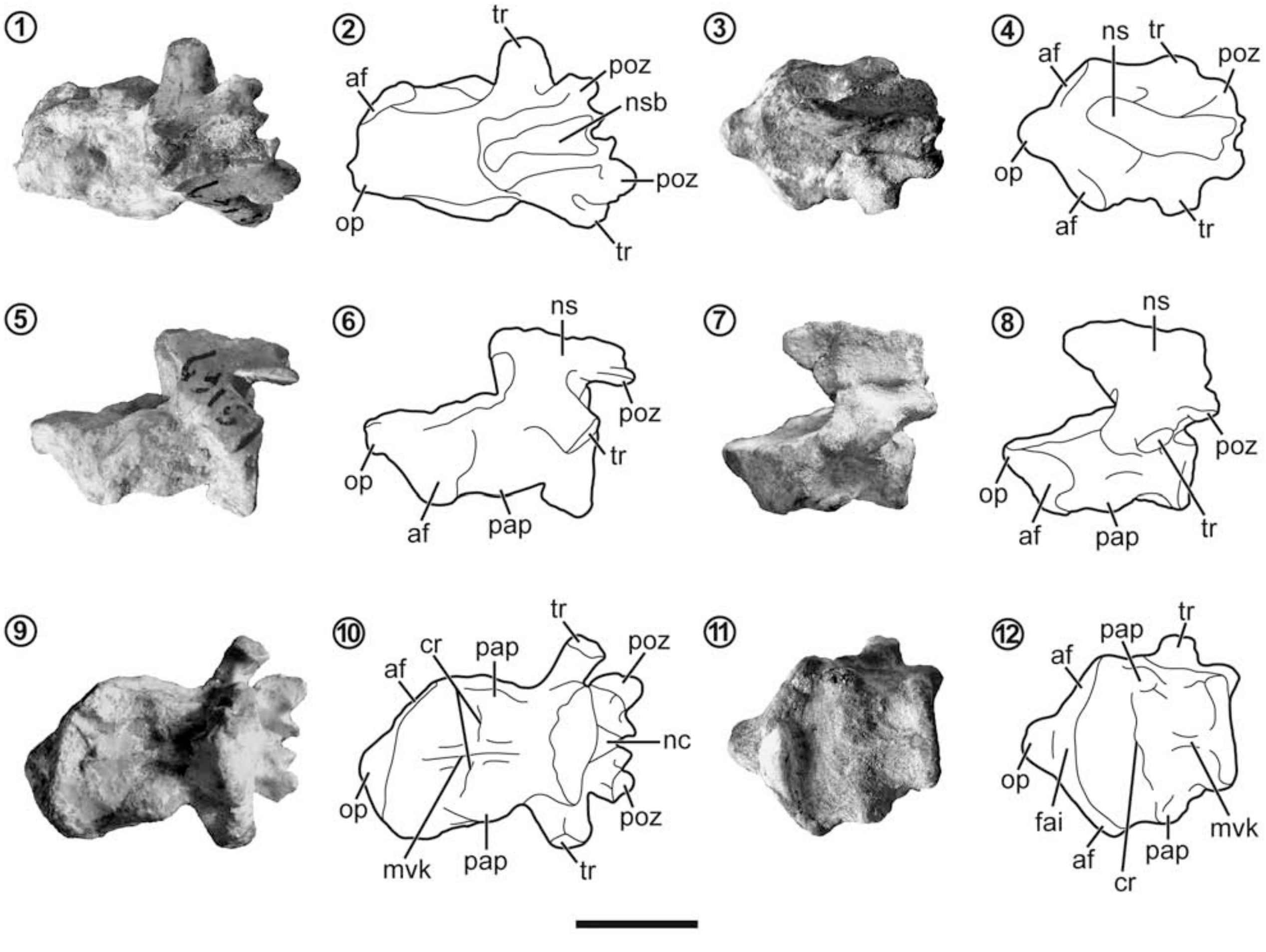

1
2
tr
af
poz
nsb
poz
op
tr
3
4
ns
tr
af
poz
op
af
tr
5
6
ns
poz
tr
op
af
pap
7
8
ns
poz
op
af
pap
tr
9
10
tr
cr
pap
af
poz
nc
op
poz
mvk
pap
tr
11
12
tr
pap
af
op
fai
mvk
af
pap
cr

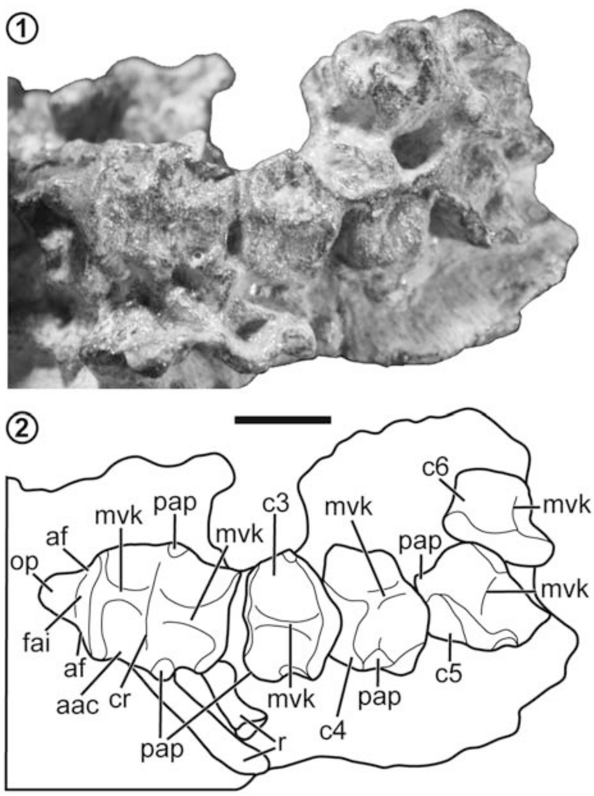

1
2
c6
mvk
mvk
pap
c3
mvk
pap
mvk
af
op
mvk
fai
af
aac
cr
pap
mvk
r
c4
pap
c5

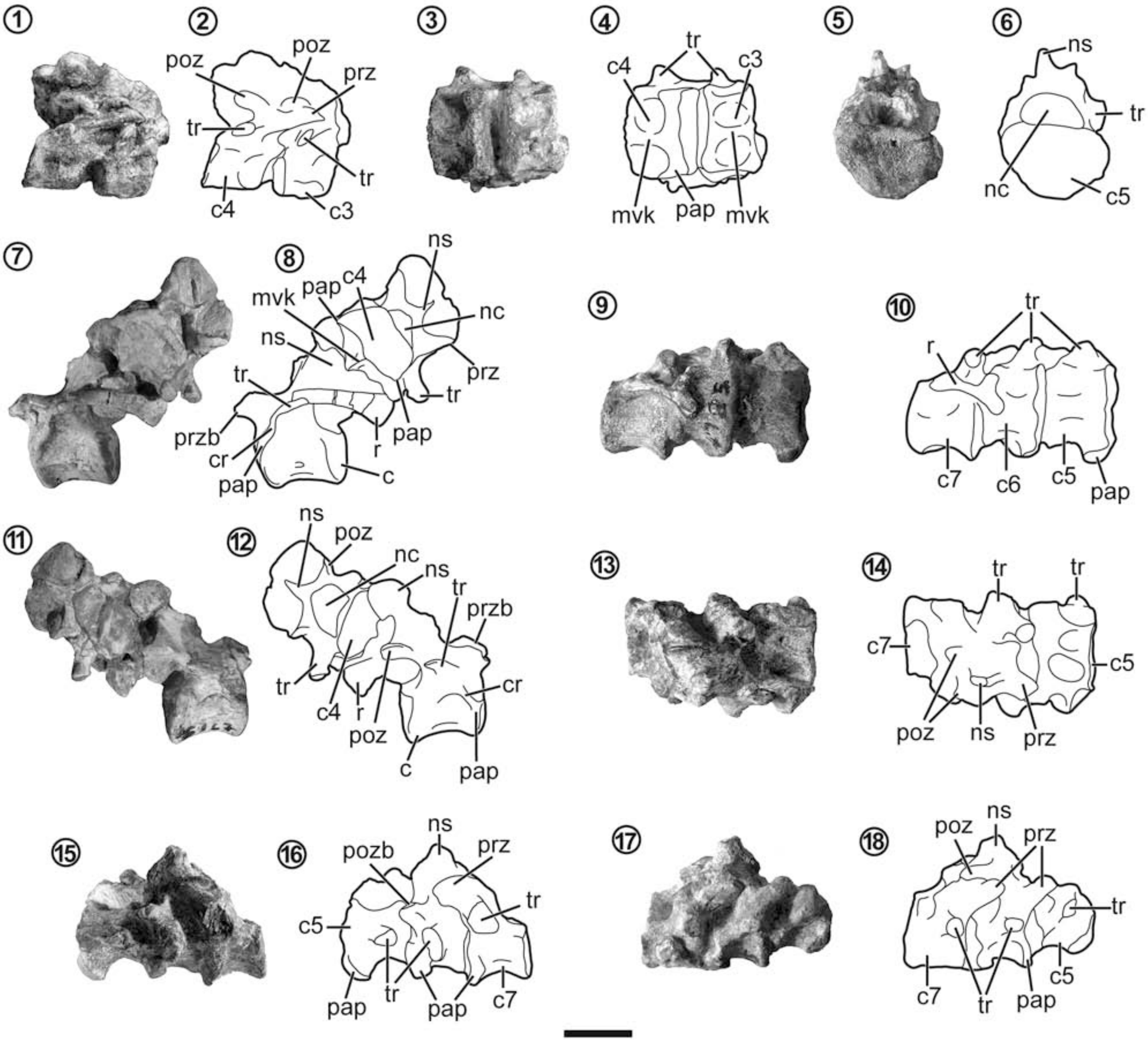
1
2
poz
poz
prz
tr
tr
c4
c3
3
4
tr
c4
c3
mvk
pap
mvk
5
6
ns
tr
nc
c5
7
8
ns
pap
c4
mvk
nc
ns
prz
tr
tr
przb
cr
pap
r
pap
c
9
10
tr
r
c7
c6
c5
pap
11
12
ns
poz
nc
ns
tr
przb
tr
c4
r
cr
poz
c
pap
13
14
tr
tr
c7
c5
poz
ns
prz
15
16
ns
pozb
prz
tr
c5
tr
pap
pap
c7
17
18
poz
ns
prz
tr
c7
tr
pap
c5

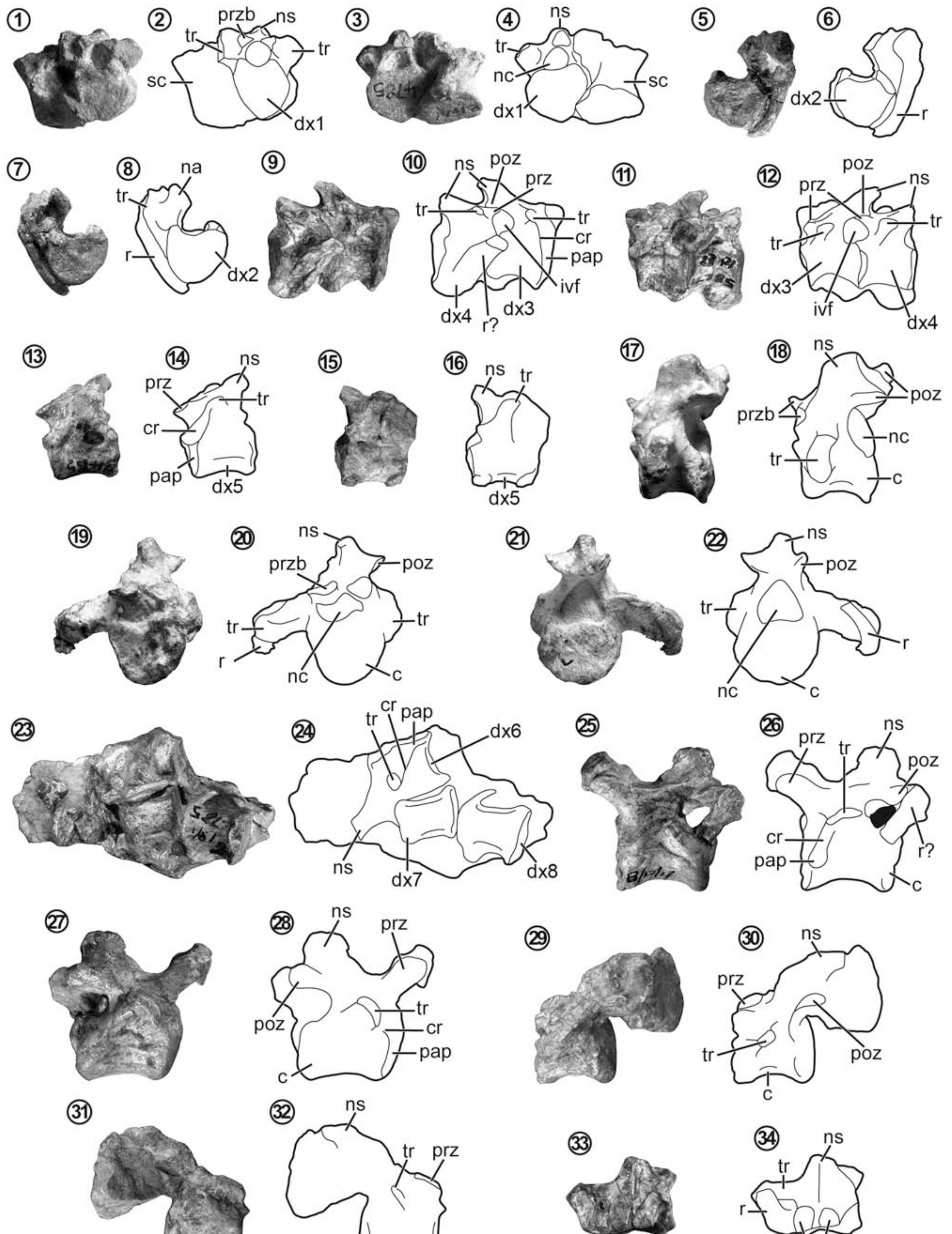
1
2
przb
ns
tr
tr
sc
dx1
3
4
ns
tr
nc
sc
dx1
5
6
dx2
r
7
8
na
tr
r
dx2
9
10
ns
poz
prz
tr
tr
cr
pap
ivf
dx4
r?
dx3
11
12
poz
prz
ns
tr
tr
dx3
ivf
dx4
13
14
ns
prz
tr
cr
pap
dx5
15
16
ns
tr
dx5
17
18
ns
poz
przb
nc
tr
c
19
20
ns
poz
przb
tr
tr
r
nc
c
21
22
ns
poz
tr
r
nc
c
23
24
cr
tr
pap
dx6
ns
dx7
dx8
25
26
ns
prz
tr
poz
cr
r?
pap
c
27
28
ns
prz
tr
poz
cr
pap
c
29
30
ns
prz
poz
tr
c
31
32
ns
tr
prz
c
33
34
ns
tr
r
prz

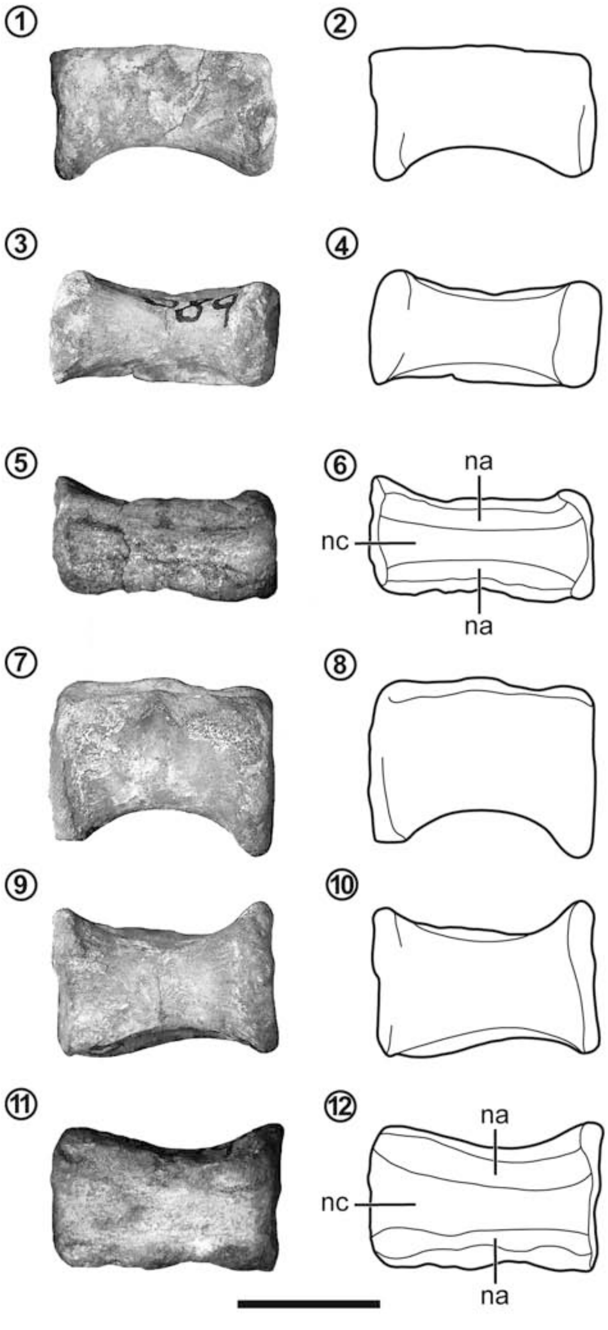

①
②
③
④
⑤
⑥
na
nc
na
⑦
⑧
⑨
⑩
⑪
⑫
na
nc
na

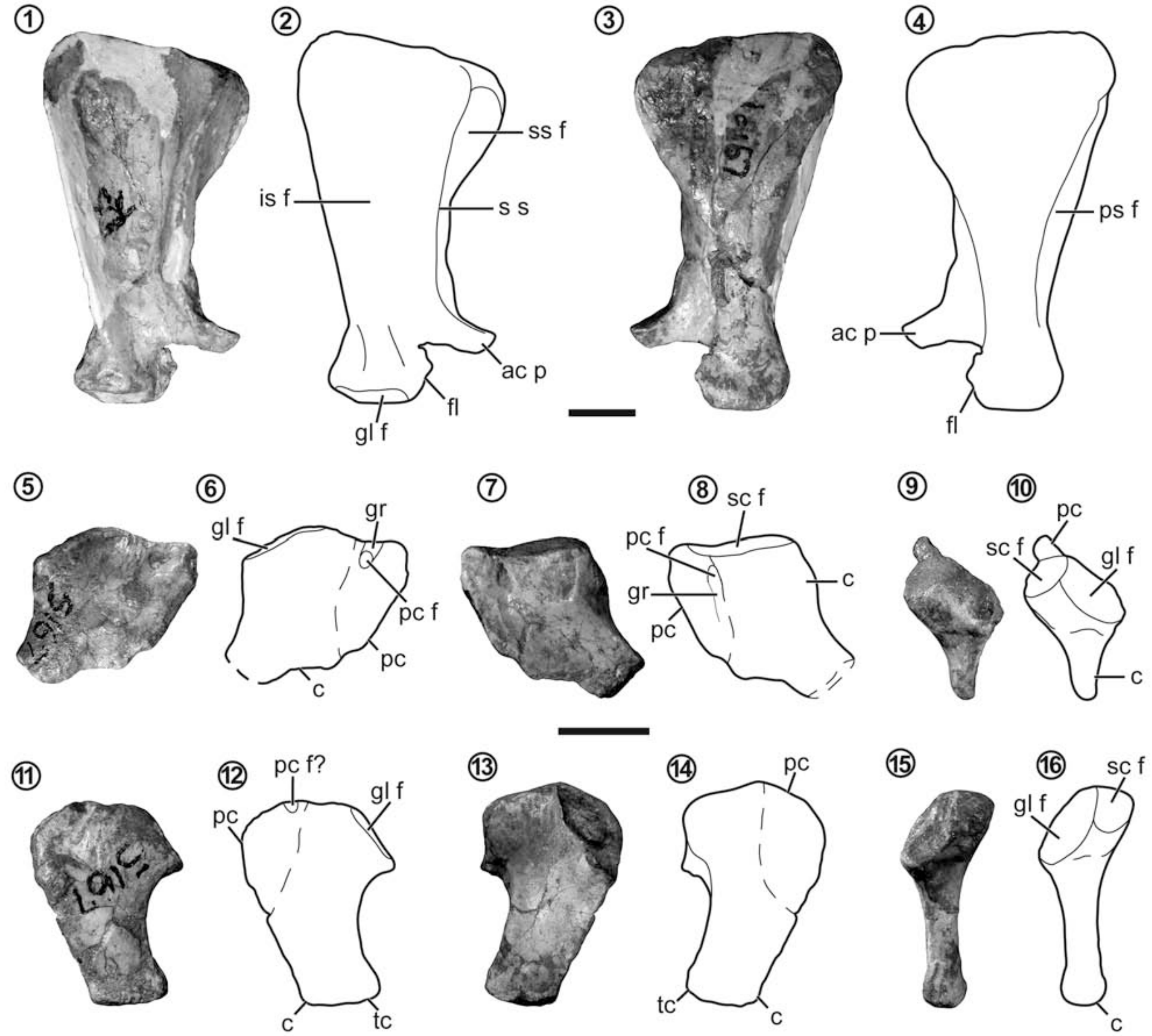

1
2
3
4
ss f
is f
s s
ps f
ac p
fl
gl f
5
6
7
8
9
10
gl f
gr
pc f
pc
c
sc f
pc f
gr
pc
c
pc
sc f
gl f
c
11
12
13
14
15
16
pc f?
pc
gl f
c
tc
pc
tc
c
sc f
gl f
c

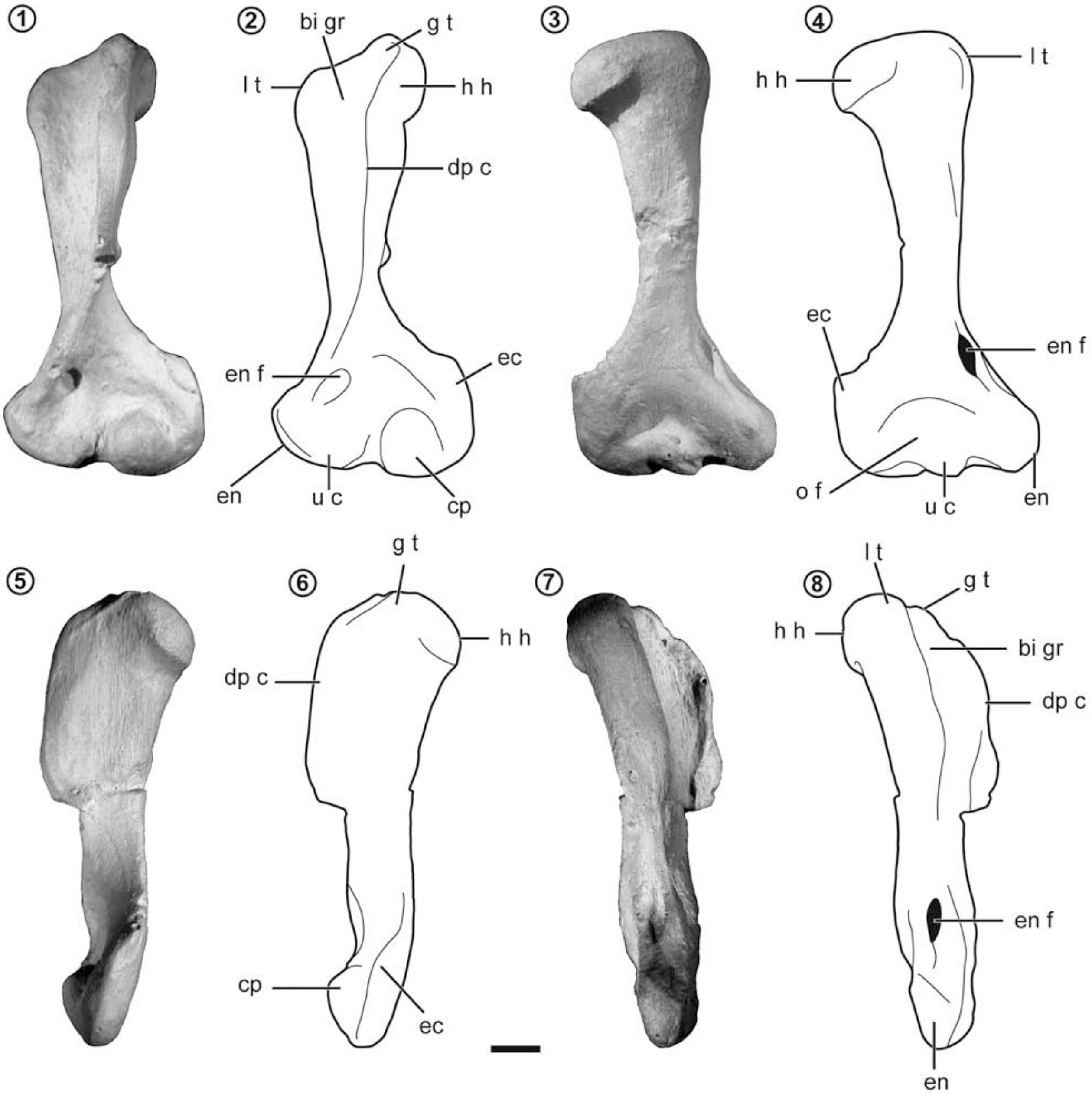

1
2
bi gr
g t
l t
h h
dp c
en f
ec
en
u c
cp
3
4
l t
h h
ec
en f
o f
u c
en
5
6
g t
h h
dp c
cp
ec
7
8
l t
g t
h h
bi gr
dp c
en f
en

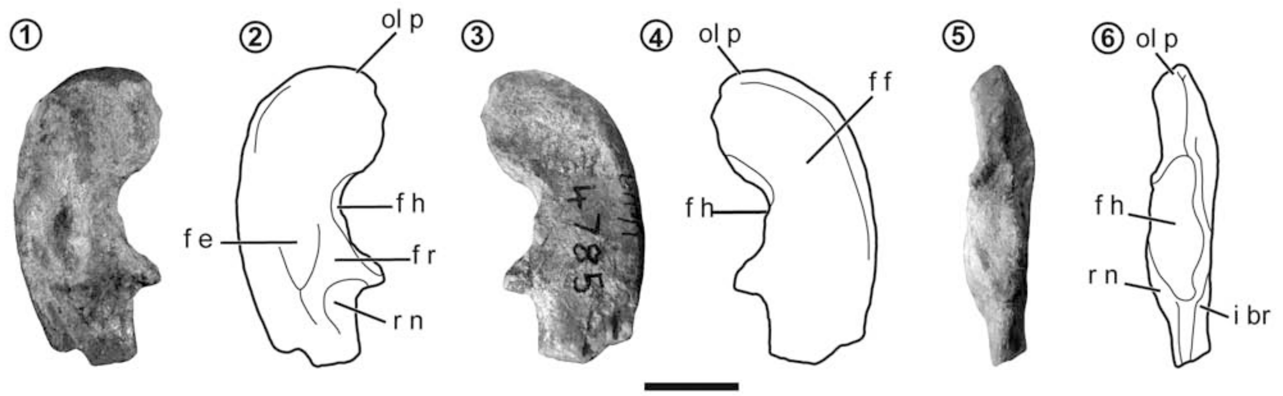

1
2
ol p
f h
f e
f r
r n
3
4785
4
ol p
f f
f h
5
6
ol p
f h
r n
i br

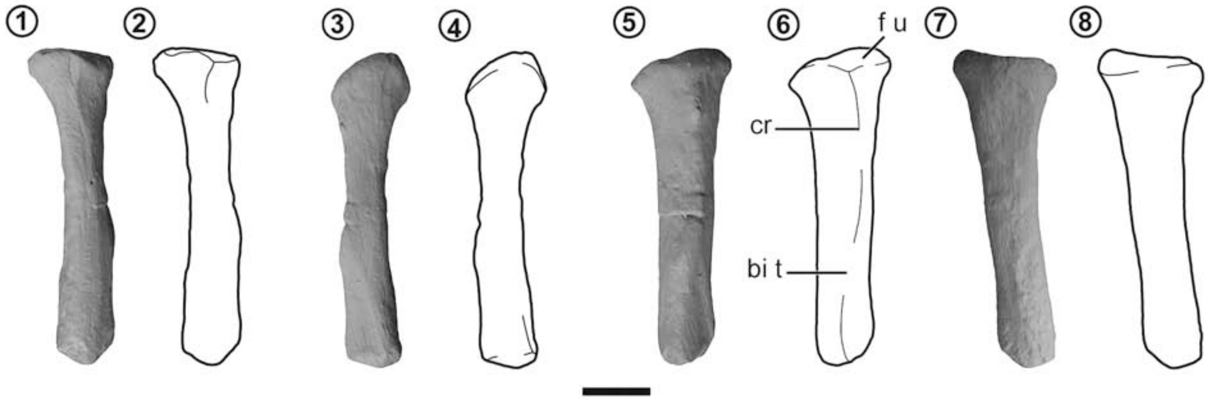

①
②
③
④
⑤
⑥
f u
cr
bi t
⑦
⑧

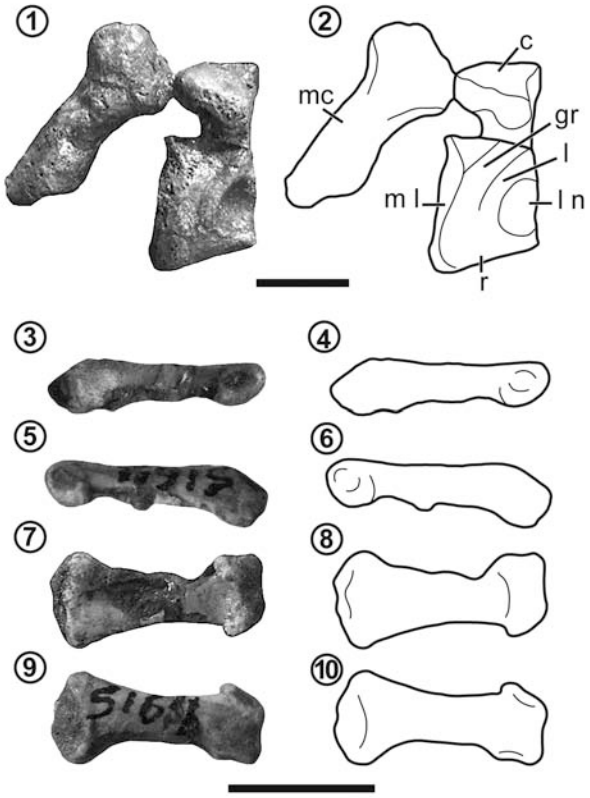

1
2
c
mc
gr
l
m l
l n
r
3
4
5
6
7
8
9
10

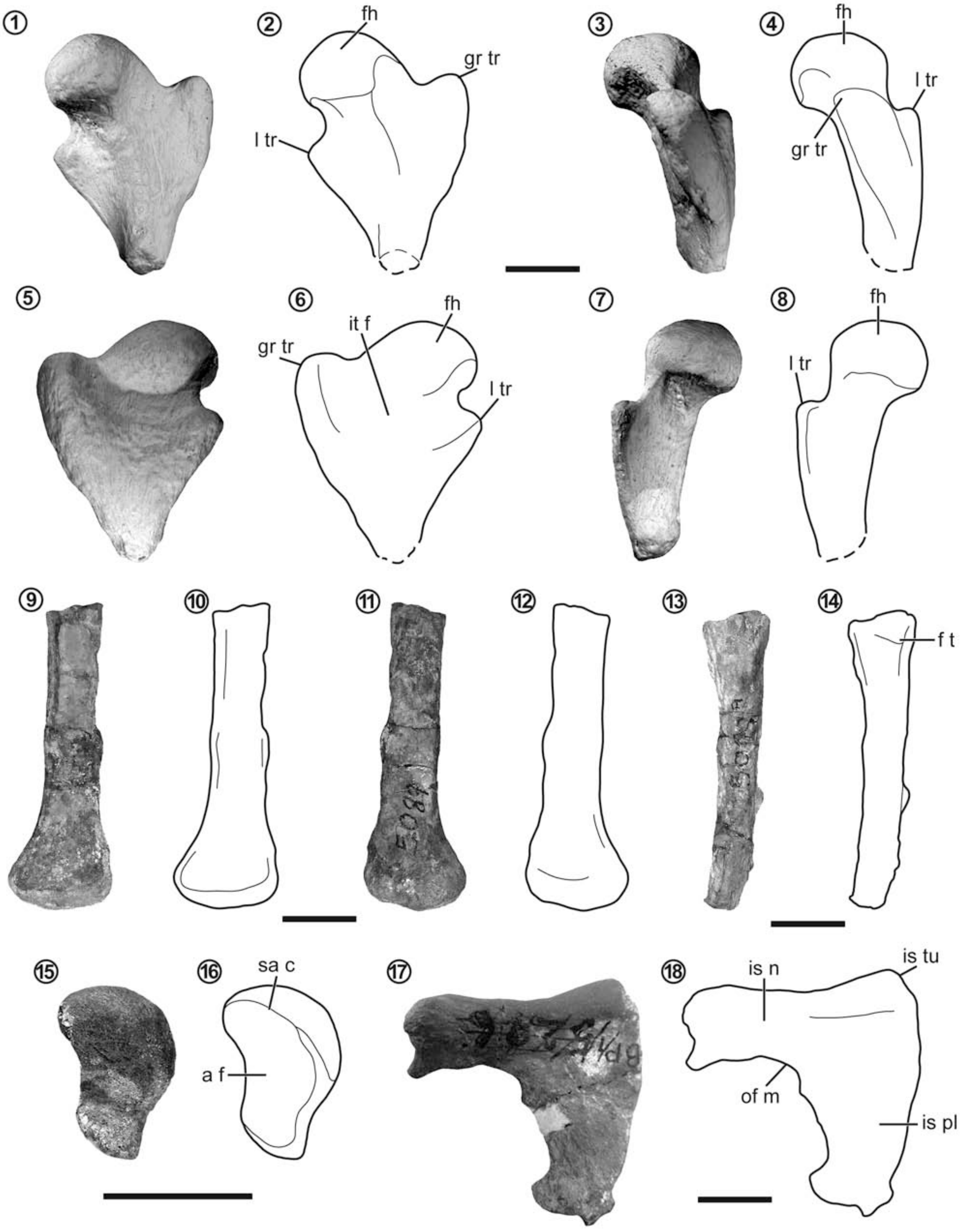

①
②
fh
gr tr
l tr
③
④
fh
l tr
gr tr
⑤
⑥
it f
fh
gr tr
l tr
⑦
⑧
fh
l tr
⑨
⑩
⑪
⑫
⑬
⑭
f t
⑮
⑯
sa c
a f
⑰
⑱
is n
is tu
of m
is pl

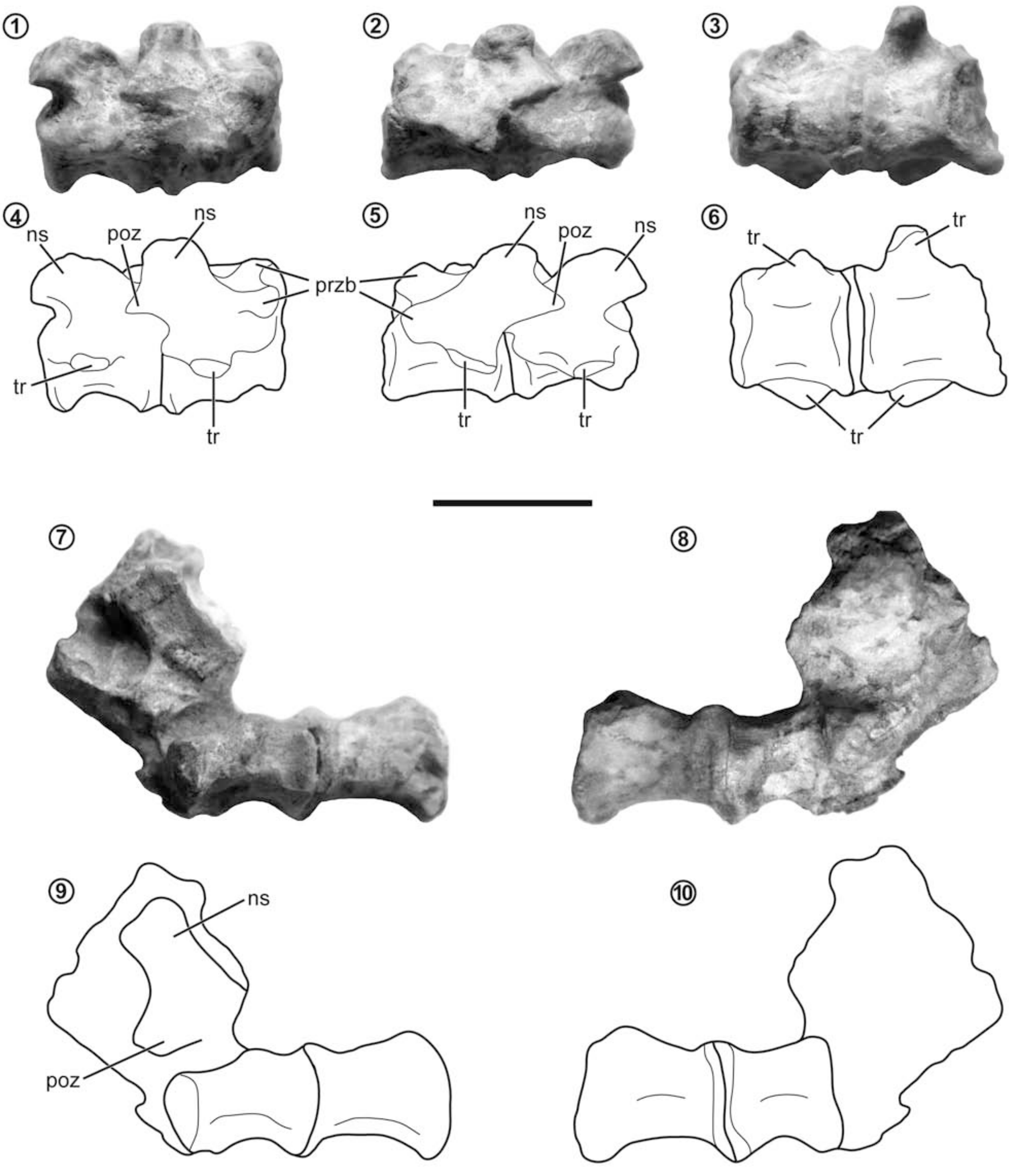

1
2
3
4
5
6
ns
poz
ns
przb
ns
poz
ns
tr
tr
tr
tr
tr
tr
tr
7
8
9
10
ns
poz

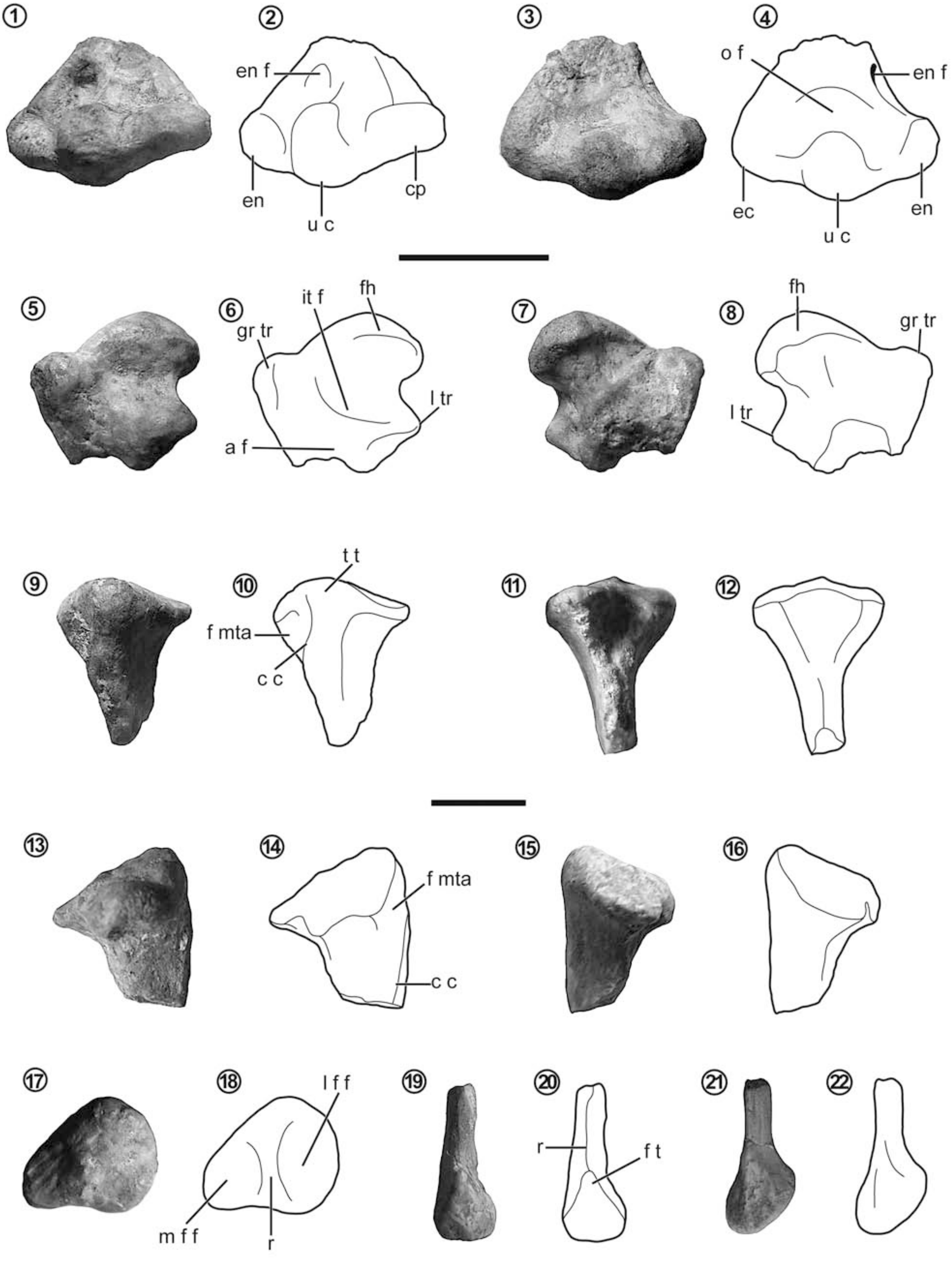
①
②
en f
en
u c
cp
③
④
o f
en f
ec
u c
en
⑤
⑥
it f
fh
gr tr
l tr
a f
⑦
⑧
fh
gr tr
l tr
⑨
⑩
t t
f mta
c c
⑪
⑫
⑬
⑭
f mta
c c
⑮
⑯
⑰
⑱
l f f
m f f
r
⑲
⑳
r
f t
㉑
㉒

Table 1 – Recognized tritylodontid taxa

	Recorded elements	Relative abundance	Age	Region	Maximum skull length
Bienotherium magnum	*Skull*	*Rare*	*Sinnemurian - Pliensbachian*	*China*	*–*[1]
Bienotherium yunnanense	*Skull, postcranium*	*Common*	*Hettangian - Sinnemurian*	*China*	*121*
Bienotheroides shartegensis	*Skull, lower jaw*	*Rare*	*Late Jurassic*	*Mongolia*	*~105*
Bienotheroides ultimus	*Skull, postcranium*	*Rare*	*Oxfordian*	*China*	*–*
Bienotheroides wanhsienensis	*Skull, lower jaw, postcranium*	*Common*	*Middle-Late Jurassic*	*China*	*107*
Bienotheroides zigongensis	*Skull, lower jaw, postcranium*	*Common*	*Bathonian - Callovian*	*China*	*112*
Bocatherium mexicanum	*Skull*	*Rare*	*Early-?Middle Jurassic*	*Mexico*	*51*
Dianzhongia longirostrata	*Skull*	*Rare*	*Sinnemurian - Pliensbachian*	*China*	*75*
Dinnebitodon amarali	*Skull, postcranium*	*Intermediate*	*Sinnemurian - Pliensbachian*	*United States*	*~110*[2]
Kayentatherium wellesi	*Skull, lower jaw, postcranium*	*Common*	*Sinnemurian - Pliensbachian*	*United States*	*260*
Lufengia delicata	*Skull*	*Rare*	*Sinnemurian - Pliensbachian*	*China*	*47*
Montirictus kuwajimaensis	*Fragmentary skull bones, lower jaw, isolated teeth*	*Rare*	*Barremian–Aptian*	*Japan*	*–*
Oligokyphus lufengensis	*Lower jaw*	*Rare*	*Hettangian - Sinnemurian*	*China*	*–*[3]
Oligokyphus major	*Skull, postcranium*	*Common*	*?Pliensabachian*	*United Kingdom*	*~90*
Oligokyphus *sp*.	*Skull, lower jaw*	*Intermediate*	*Sinnemurian - Pliensbachian*	*United States*	*~24 (juvenile)*
Oligokyphus triserialis	*Isolated teeth*	*Rare*	*Late Norian - Hettangian*	*Germany*	*–*
Stereognathus ooliticus	*Skull*	*Rare*	*Middle Jurassic*	*United Kingdom*	*–*
Tritylodon longaevus	*Skull, lower jaw, postcranium*	*Common*	*Hettangian*	*South Africa*	*130*
Tritylodontidae	*Isolated teeth*	*Rare*	*Barremian–Aptian*	*Japan*	*–*
Tritylodontidae	*Isolated teeth*	*Rare*	*Sinnemurian Pliensbachian*	*Antartica*	*–*

Tritylodontoideus maximus	*Skull, lower jaw, postcranium*	*Rare*	*Hettangian*	*South Africa*	*250*
Xenocretosuchus kolossovi	*Isolated teeth*	*Rare*	*Upper Jurassic – Lower Cretaceous*	*Russia*	–
Xenocretosuchus sibiricus	*Isolated teeth*	*Rare*	*Barremian - Aptian*	*Russia*	–
Yuanotherium minor	*Maxilla with teeth*	*Rare*	*Oxfordian*	*China*	–
Yunnanodon brevirostre	*Skull*	*Rare*	*Sinnemurian - Pliensbachian*	*China*	*37*

Measurements in millimeters. [1] *Cheek-teeth row is 76 mm long, almost twice that of B. yunannense (Chow, 1962);* [2] *Estimated after figure 1 of Sues (1986);* [3] *Horizontal ramus length (from the anterior end of the dentary to the posterior end of the third postcanine; a fourth postcanine is preserved but out of place) ~20 mm.*

***Table 2** – Available* **Tritylodon** *specimens*

Specimen number	Recorded elements	Basal skull length	Locality
BP/1/4778	*Skull, lower jaw, proximal femur, unprepared isolated vertebrae, and left and right fragmentary scapulae.*	*129*	*Upper Elliot Formation, Farm Saaihoek, 310, Fouriesburg, Free State Province, South Africa*
BP/1/4782	*Skull, right dentary, atlas-axis, a postaxial cervical vertebra (c4?), and three dorsal vertebrae.*	*~97*	*Upper Elliot Formation, Farm Bloemhoek 330, Fouriesburg, Free State Province, South Africa*
BP/1/4783	*Proximal and distal portion of femur (cast).*	–	*Upper Elliot Formation, Farm Bloemhoek 330, Fouriesburg, Free State Province, South Africa*
BP/1/4785	*Five postaxial cervical vertebrae (c3-c7), 13 dorsal vertebrae, glenoid portion of left scapula, proximal and distal portion of right humerus (cast), left humerus (cast), proximal portion of left ulna, and fragmentary ribs, and undeterminable fragments.*	–	*Upper Elliot Formation, unknown locality, South Africa.*
BP/1/4965	*Partial skull and lower jaw, and first seven articulated cervical vertebrae.*	*~140*	*Upper Elliot Formation, Farm Twee Zusters 251, Ladybrand, Free State Province, South Africa*
BP/1/4976	*Skull, lower jaws, and part of the autopodium.*	*~130*	*Upper Elliot Formation, Farm Nova Barletta 307, Clocolan, Free State Province, South Africa.*
BP/1/5089	*Fragmentary posterior portion of the right lower jaw, a dorsal vertebra, two caudal vertebrae, left humerus (cast), proximal and distal portion of right humerus, proximal left femur (cast), fragmentary right fibula (missing distal portion), fragmentary right tibia, and indeterminable fragments.*	–	*Upper Elliot Formation, Farm Emmaus 335, Ladybrand, Free State Province, South Africa.*
BP/1/5152a	*Distal left? femur.*	–	*Upper Elliot Formation, Farm Oldenberg 45, Ladybrand, Free State Province, South Africa.*
BP/1/5167	*Skull, partial right lower jaw, fragmentary posterior portion of left lower jaw, atlas-axis, a postaxial cervical vertebra (c4?), six dorsal vertebrae, distal femur, right scapula, right and left coracoid and procoracoid, left radius (cast) missing the distal portion, a phalange, and indeterminable fragments.*	*121*	*Upper Elliot Formation, Farm Bramleyshoek 52, Bethlehem, Free State Province, South Africa.*
BP/1/5269	*Partial skull and right ischium.*	*~125*	*Upper Elliot Formation, Farm Damplaats 55, Ladybrand, Free State Province, South Africa.*
BP/1/5305	*Fragments of lower jaw and proximal portion of left femur*	–	*Upper Elliot Formation, Farm Damplaats 55, Ladybrand, Free State Province, South Africa.*
BP/1/5516	*Proximal portions of right and left femurs.*	–	*Upper Elliot Formation, Farm Mequatling 278, Clocolan, Free State Province, South Africa.*
BP/1/5671	*Proximal and distal portions of left femur (casts) and left humerus (cast).*	–	*Upper Elliot Formation, Clarens townlands, Clarens, Free State Province, South Africa.*

Measurements in millimeters.

TABLE 3 – Body mass estimations for tritylodontid taxa for which postcranial elements are known

	Skeletal proxy	*Measurement*	*Estimated mass*
Bienotherium yunnanense	*Maximum skull length*	*121*	*8.5kg*
Bienotheroides ultimus	*Humerus length*	*63.6*	*1.5kg*
Bienotheroides wanhsienensis	*Maximum skull length*	*107*	*5.8kg*
Bienotheroides zigongensis	*Maximum skull length*	*112*	*6.7kg*
Dinnebitodon amarali	*Maximum skull length*	*110*[1]	*6.3kg*
Kayentatherium wellesi	*Maximum skull length*	*260*	*93.1kg*
Oligokyphus major	*Maximum skull length*	*90*	*3.4kg*
Tritylodon longaevus	*Maximum skull length*	*130*	*10.6kg*
Tritylodontidae[2]	*Femoral length*	*95*	*3.2kg*
Tritylodontoideus maximus	*Maximum skull length*	*250*	*82.3kg*

Measurements in millimeters. [1] Estimated after figure 1 of Sues (1986); [2] Indeterminate tritylodontid partial skeleton (CXPM C2019 2A235) from the Lufeng Formation (Lower Jurassic), China.

***Table 4 – Available vertebrae of* Tritylodon longaevus**

	Lettering	Mode of occurrence	Description/interpretation
4782	–	*Isolated vertebra*	*Atlas-axis*
	b	*Isolated vertebra*	*c4*
	c	*Isolated vertebra*	*dorsal, posterior to dx8*
	d	*Isolated vertebra*	*anterior dorsal (dx5?)*
4785	*a*	*Two articulated vertebrae*	*c3–4*
	b	*Two articulated vertebrae*	*c5–7*
	c	*Isolated vertebra associated with a scapular fragment*	*dx1*
	d	*Isolated vertebra*	*dx2*
	e	*Two articulated vertebrae*	*dx3–4*
	f	*Isolated vertebra*	*dx5*
	g	*Isolated vertebra*	*posterior dorsal*
	h	*Isolated vertebra*	*dorsal, posterior to dx8*
	i	*Isolated vertebra*	*dorsal, posterior to dx8*
	j	*Block with three associated vertebrae*	*dx6–8*
4965	–	*Block with five articulated vertebrae*	*Atlas-axis and c3–6*
5089	–	*Isolated vertebra*	*dorsal, posterior to dx8*
	a	*Isolated vertebra*	*caudal*
	b	*Isolated vertebra*	*caudal*
5167	–	*Isolated vertebra*	*Atlas-axis*
	b	*Isolated vertebra*	*anterior dorsal (dx1-4?)*
	d	*Block with two associated vertebrae*	*dx1-4? and a dorsal posterior to dx8*
	e	*Isolated vertebra*	*dorsal, posterior to dx8*
	x	*Block with two associated vertebrae*	*c4 and a dorsal posterior to dx8*
	z	*Isolated vertebra*	*anterior dorsal (dx3–4?)*

***TABLE 5- Measurements (in millimeters) of vertebral centra of* Tritylodon**		
Specimen	**Length**	**Width**
BP/1/4782a (atlas-axis centrum)	*14.8*	*7.9*
BP/1/4782b (c4)	*5.9*	*8.5*
BP/1/4782d (anterior dorsal, dx5?)	*10.8*	*9.4*
BP/1/4782c (dorsal, posterior to dx8)	*13.3*	*11.4*
BP/1/4785a (c3)	*6.6*	*11.3*
BP/1/4785a (c4)	*7.3*	*12.3*
BP/1/4785b (c5)	*7.9*	*11.6*
BP/1/4785b (c6)	*8*	*11.8*
BP/1/4785b (c7)	*8.8*	*11.2*
BP/1/4785c (dx1)	*8.9*	*11.5*
BP/1/4785d (dx2)	*9*	*11.6*
BP/1/4785e (dx3)	*9.5*	*10.3*
BP/1/4785e (dx4)	*10*	*10.3*
BP/1/4785f (dx5)	*10.4*	*9.9*
BP/1/4785j (dx6)	*10.6*	*10*
BP/1/4785j (dx7)	*11.7*	*10.5*
BP/1/4785j (dx8)	*12*	*11.4*
BP/1/4785h (dorsal, posterior to dx8)	*16.2*	*13.1*
BP/1/4785i (dorsal, posterior to dx8)	*15.3*	*13.8*
BP/1/4785g (posterior dorsal)	*10.6*	*10.4*
BP/1/4965 (atlas-axis centrum)	*22.1*	*13.2*
BP/1/4965 (c3)	*11*	*14*
BP/1/4965 (c4)	*9.6*	*12.6*
BP/1/4965 (c5)	*9.8*	*13.3*
BP/1/4965 (c6)	*7.6*	*11.2*
BP/1/5089 (dorsal, posterior to dx8)	*12.1*	*9.4*
BP/1/5089a (caudal)	*15.3*	*10.2*
BP/1/5089b (caudal)	*15.2*	*7.6*
BP/1/5167a (atlas-axis centrum)	*17.9*	*8.7*
BP/1/5167x (c4)	*6.4*	*10*
BP/1/5167b (anterior dorsal)	*10.6*	*12.9*
BP/1/5167d (anterior dorsal)	*8.3*	*10*
BP/1/5167z (anterior dorsal, dx3-4?)	*8.1(broken)*	*8*
BP/1/5167d (dorsal, posterior to dx8)	*11.1*	*9.3*
BP/1/5167x (dorsal, posterior to dx8)	*12.4*	*10.5*
BP/1/5167e (dorsal, posterior to dx8)	*12*	*8 (distorted)*

Table 6 – Proportions of the humerus

	DiaL	*PW*	*DW*
Bienotheroides ultimus[1]	*24%*	*44%*	*52%*
Bienotherium[2]	*30%*	*48%*	*57%*
Cynognathus	*18%*[3]	*33 – 42%*[4]	*39 – 52%*[4]
Kayentatherium wellesi[5]	*24%*	*44%*	*50%*
Oligokyphus major[6]	*30%*	*30%*	*47%*
Thrinaxodon	*18%*[3]	*32%*[4]	*49%*[4]
Tritylodon longaevus	*10*[7] *– 17*[8]*%*	*34*[7] *– 40*[8]*%*	*48*[7] *– 51*[8]*%*

DiaL, proportion of the diaphysis length relative to the length of the humerus. PW, proportion of the maximum width of the proximal region relative to the length of the humerus. DW, proportion of the maximum width of the distal region relative to the length of the humerus. The length of the diaphysis was measured from the distal inflexion of the deltopectoral crest to the proximal rim of the entepicondylar foramen. [1] *Proportions calculated from the illustrations of Maisch et al., 2004;* [2] *Proportions calculated from the measurements and illustrations of Young, 1947;* [3] *Calculated from the figures of Jenkins, 1971;* [4] *From Abdala, 1999;* [5] *Proportions calculated from the measurements provided by Sues and Jenkins, 2006 and from the personal analysis of specimen MCZ8812;* [6] *Proportions calculated from the measurements and illustrations of Kühne, 1956;* [7] *Calculated from specimen BP/1/5671;* [8] *Calculated from specimen BP/1/4785.*